Applied Energy 361 (2024) 122921

Contents lists available at ScienceDirect

Applied Energy

journal homepage: www.elsevier.com/locate/apenergy

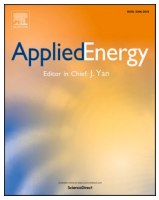

A techno-economic assessment of two recycling processes for black mass from end-of-life lithium-ion batteries

Richard Woeste [a,*], Emanuel-Sebastian Drude [b], Dzeneta Vrucak [b], Kai Klöckner [a], Elinor Rombach [b], Peter Letmathe [a], Bernd Friedrich [b]

[a] Chair of Management Accounting, RWTH Aachen University, Templergraben 64, 52062 Aachen, Germany
[b] Institute for Process Metallurgy and Metal Recycling, RWTH Aachen University, Intzestraße 3, 52056 Aachen, Germany

HIGHLIGHTS

- Consideration of new method for early-stage lithium recovery before hydrometallurgy.
- Current LIB cell chemistries pose challenges to profitable LIB recycling.
- Main factors affecting economic feasibility are material and energy prices.
- Hydrometallurgy found to be more robust against changing boundary conditions.
- Upscaling of mass throughput is expected to increase profitability of processes.

ARTICLE INFO

Keywords:
Electromobility
lithium-ion battery (LIB) recycling
Circular economy
Total cost of ownership (TCO) analysis
Pyrometallurgical recycling
Hydrometallurgical recycling

ABSTRACT

Against the background of the growing market share of electric vehicles worldwide, the recycling of used vehicle batteries needs to be further investigated. In this paper, two recycling processes for pyrolyzed black mass from end-of-life lithium-ion batteries, a pyrometallurgical route and a hydrometallurgical route with precedent early-stage lithium recovery, are techno-economically evaluated using a total cost of ownership approach. From a technical point of view, this approach thus focuses on maximizing the recycling efficiency achieved by pyrolysis treatment of the battery scrap to pre-separate copper and aluminum. A scenario analysis of the future development of material prices and the market share of cell chemistries is performed to determine the influence of these variables on the profitability of the recycling processes. In general, current trends in cell chemistry pose challenges to profitable LIB recycling. The hydrometallurgical recycling route was found to be less susceptible to price fluctuations and changes in cell chemistry than the pyrometallurgical recycling route and is therefore expected to be more profitable than the pyrometallurgical recycling route when scaled up, especially considering the trend towards decreasing cobalt content in lithium-ion batteries.

1. Introduction

Lithium-ion batteries (LIB) play an important role in climate protection and the necessary decarbonization of energy supply, transport, and mobility [10,26]. The global battery market is expected to grow strongly in the coming years due to the growing electromobility and stationary energy storage market [62,68,76,77,79]. This will lead to a corresponding number of end-of-life LIBs. Directive 2006/66/EC regulates waste management in relation to batteries and sets EU-wide collection targets and recycling requirements [35]. Accordingly, a

Abbreviations: BEHG, Fuel Emissions Trading Act (Germany); BM, Black mass; DERA, German Mineral Resources Agency; EG8/9, Pay groups 8/9 according to collective agreement (Germany); ESLR, Early-stage lithium recovery; EU-ETS, European Emissions Trading Scheme; HE-NMC, High-energy NMC; HVS, High-voltage spinel; ICP-OES, Inductively coupled plasma-optical emission spectrometer; LCO, Lithium cobalt oxide; LFP, Lithium iron phosphate; LIB, Lithium-ion battery; LMO, Lithium manganese oxide; NCA, Lithium nickel cobalt aluminum oxide; nEHS, National Emissions Trading Scheme (Germany); NMC, Lithium nickel manganese cobalt oxide; NPV, Net present value; OLS, Ordinary least squares; SSB, Solid-state battery; TCO, Total cost of ownership; USGS, United States Geological Survey; WACC, Weighted average cost of capital.

* Corresponding author.
E-mail address: woeste@controlling.rwth-aachen.de (R. Woeste).

https://doi.org/10.1016/j.apenergy.2024.122921
Received 1 December 2023; Received in revised form 7 February 2024; Accepted 23 February 2024
Available online 1 March 2024

recycling efficiency of at least 50% of the average battery weight is mandatory. New EU regulations are planned that will require even higher recovery rates of up to 80% by 2031 [39]. There are also efforts in the USA and China to promote recycling of LIBs, although these are less stringent than the EU requirements [33,44].

Recycling targets are not only motivated by environmental concerns. Rather, limited raw material resources and geopolitical risks combined with rapidly increasing raw material demand are also key reasons for the strong recycling efforts [14,15,48]. Several studies by the European Commission, the United States Geological Survey (USGS), and the German Mineral Resources Agency (DERA) point to supply risks for key raw materials for LIB manufacturing, such as cobalt, lithium, and graphite [15,38,48,58,70]. Even for raw materials not considered critical, such as copper or nickel [48], recycling helps to reduce the unnecessary mining of additional raw materials by using materials already in circulation more efficiently.

Due to the fact that no standardized process chain has yet been determined [51], various approaches to recycling end-of-life LIBs have been described in the literature. Typically, the objective is to recover valuable materials from LIBs, particularly from the active materials in the anode and cathode, using pyrometallurgical and/or hydrometallurgical processes with pretreatments as appropriate [50,65]. Fujita et al. [43] and Mossali et al. [64] specify various recycling options for LIBs and review the different methods in more detail. Blömeke et al. [7] describe in their study three different approaches: a pyrometallurgical, a mechanical and a hybrid recycling route for exemplary industrially scaled LIBs recycling options. Besides the more conventional routes, which are mainly pyrometallurgical or hydrometallurgical, direct recycling options differ from these in that they aim at regenerating battery materials rather than breaking down their chemical structure [65]. As an alternative to recycling, end-of-life LIBs can be reused in different applications, for example, stationary energy storage systems [64]. Lander et al. [57] provide insights into the disassembly costs of LIBs depending on the battery pack design. Gutsch and Leker [49] present findings on the cost structure of battery production with an outlook on the effects of incorporating recycled materials.

Although literature provides exhaustive information on various approaches for recycling LIBs, a detailed economic evaluation of these processes comparing a pyrometallurgical and a hydrometallurgical recycling route is still pending. Reinhart et al. [67] conducted a similar economic evaluation of two pyrometallurgical recycling processes. The motivation for this work is to close this research gap. For this purpose, two competing recycling processes for LIBs are economically evaluated at a pre-industrial level using a total cost of ownership (TCO) approach. While one process follows a pyrometallurgical approach, the other route uses a hydrometallurgical process, including a pretreatment for early-stage lithium recovery (ESLR). It is assumed that the profitability of the recycling processes depends substantially on the prices, quantity, and type of the raw materials recovered. The research questions to be answered are:

(1) *What are factors influencing the economic advantageousness of the two recycling processes?*
(2) *How could possible future developments influence the result of the economic evaluation?*

This paper first provides a brief overview of both processes from a technical point of view and an introduction to the evaluation methods used for the economic evaluation. Subsequently, the market prices of materials and process auxiliaries, as well as the composition of common LIB types, are analyzed, and the TCO model used is explained in detail. The TCO for both processes per amount of pyrolyzed black mass from end-of-life LIBs are then calculated for different price and cell chemistry market scenarios. The values obtained here form the basis for the core contribution of this work – the economic evaluation and comparison of the two recycling process routes. To account for external costs of greenhouse gas emissions, CO_2 prices are included in the sensitivity analysis. The paper concludes with a discussion of the results and limitations as well as an outlook on the influence of future battery developments.

2. Material and methods

In this section, the two recycling processes that are to be evaluated economically are presented and described from a technical point of view. In addition, the economic evaluation methods used later in this thesis are briefly explained.

2.1. Evaluated recycling processes from a technical point of view

This section briefly overviews the recycling processes considered in this article. Specifically, a pyrometallurgical process is compared to a hydrometallurgical process combined with a precedent ESLR step. Since both processes use pyrolyzed black mass as their primary input, the respective pretreatments of end-of-life LIBs are the same. After the spent LIBs are discharged and disassembled, they undergo thermal pretreatment. This is a pyrolysis process conducted at a temperature of 600 °C, during which the cells are deactivated, and the organic compounds are removed [71,82]. Subsequent mechanical comminution and separation, including shredding, sieving, and magnetic separation, results in four output fractions [12,42]. Cell housing, cables, screws, etc., are separated into an iron-containing scrap fraction and a non-ferrous metal scrap fraction. Anode and cathode foils are collected in a scrap fraction of copper and aluminum foil. The last fraction consists of active anode and cathode material.

In this article, only the recycling of the last fraction, hereafter referred to as pyrolyzed black mass (BM), is considered in more detail. BM primarily comprises graphite from the anode and includes various elements, such as lithium, cobalt, nickel, and manganese, from the cathode, depending on the cell chemistry. BM generally contains several impurities, including small amounts of aluminum, copper, and iron from anode and cathode foils, as well as cell housing [12,64]. Fluorine and phosphorus can be present in BM as residues from the electrolyte or separator [59].

The pyrometallurgical process is based on the description of Sommerfeld et al. [73] and aims to recover a metal alloy and a lithium-rich slag. First, the pyrolyzed black mass is pelletized using a binder. Together with quartz (SiO_2) as flux and copper(II) oxide (CuO), the pelletized BM is then processed in an electric arc furnace at a melting temperature of 1,600 °C before being poured into a mold. Considering that no pure CuO will be used on an industrial scale due to the high cost, deviating from Sommerfeld et al. [73], copper scrap with a CuO content of 30% is assumed as an input. After solidification, the metal phase and slag are separated for further processing. Alternatively, direct water-granulation of the alloy from the furnace is also conceivable. Noble metals, especially cobalt, copper, and nickel, mainly accumulate in the metal phase, while the ignoble lithium primarily passes into the slag. Besides the metal phase and slag, the pyrometallurgical process produces lithium-rich flue dust [82]. Instead of collecting and processing the flue dust, it is planned to return it to pelletization [73]. Therefore, the only outputs considered in the pyrometallurgical process are the metal alloy, the lithium-rich slag, and an off-gas containing CO_2. To obtain a plausible material flow model for the pyrometallurgical recycling process, thermodynamical modeling data provided by Sommerfeld et al. [73] is used to calculate element-based distribution coefficients that determine the distribution of each input element among the three output fractions. Elements considered for the pyrometallurgical route are aluminum (Al), graphite (as C), cobalt (Co), copper (Cu), iron (Fe), lithium (Li), manganese (Mn), nickel (Ni), silicon (Si), and oxygen (O). All elements, except carbon and oxygen, are assumed to be allocated to either the metal alloy or the slag, as flue dust is returned to the pelletizing process. The input ratio of SiO_2 and CuO are based on trials 3 and 4

from Sommerfeld et al. [73], as metal yields align with the simulated data. Table 1 provides the underlying distribution coefficients for the pyrometallurgical recycling process of the pyrolyzed black mass.

The second process path combines ESLR and hydrometallurgical processing. ESLR aims to separate lithium from black mass at an early stage to reduce impurities and complexity in subsequent process steps [71]. According to Schwich et al. [71], filtration of the black mass after being leached in water for 120 min and carbonated with supercritical CO_2 results in a filter cake containing carbon and metals such as cobalt and nickel and a lithium-rich filtrate. The filter cake still contains a small amount of lithium but is henceforth referred to as black mass without lithium. The filtrate is concentrated by boiling and re-filtering, yielding a filter cake predominantly of Li_2CO_3 with minor impurities like LiF and a residual solution of dissolved lithium compounds. Alternatively, the filtrate resulting from the initial filtration can be dried in a beaker to increase lithium yields, as no filtrate with lithium residues remains [52,86]. This study contrasts with Schwich et al. [71] in that a carbonated water leaching technique is employed for lithium recovery.

For further hydrometallurgical decomposition of the black mass without lithium, the process route described by Wang [84] is used. Initially, all graphite is extracted by leaching with HCl and H_2O_2. Subsequent copper cementation with NaOH and iron powder is followed by first iron and aluminum precipitation and then nickel, cobalt, and manganese precipitation. The residual solution obtained still contains lithium and is recirculated to reduce losses caused by saturation prior to precipitation. The recirculation process is not further investigated or considered in this study. Nevertheless, efforts can be made to recover lithium from the residual solution and conduct recirculation studies. In summary, the process yields five output fractions: graphite and copper fractions, aluminum and iron as well as nickel, cobalt, and manganese as hydroxides, and lithium as carbonate. The output fractions differ in their purity levels, with graphite being highly concentrated and aluminum/iron being less concentrated [85]. Since the hydrometallurgical process consists of multiple stages, distribution coefficients could not be determined from existing publications. Therefore, a series of experiments were conducted to determine the coefficients required for subsequent calculations. Further details regarding the experimental parameters are presented in Appendix A. Table 2 displays the distribution coefficients for the hydrometallurgical recycling process based on own experiments.

Both recycling process routes require postprocessing steps to obtain reusable materials. Lithium-rich slag from pyrometallurgy can be shredded and treated hydrometallurgically to obtain Li_2CO_3 [47,82]. However, lithium recovery from slag is rather costly [45]. Alternatively, slag can be used in the construction industry, for example, in road-making [45,50,82,83]. Metal alloys from pyrometallurgy and hydroxide outputs from hydrometallurgy can be further treated to break down these outputs into pure materials or compounds [73,85]. Graphite and Li_2CO_3 exhibit minor impurities, and both products need further refining. Li_2CO_3, for instance, requires additional purification to be suitable for reuse in battery production [4,81]. As a downgrade option, Li_2CO_3 may be utilized in the glass or ceramic industry or as a metal additive [60].

Table 1
Distribution coefficients pyrometallurgical recycling process, adapted from [73].

Element	Output in %		
	Alloy	Slag	Off-Gas
Al	2.92	97.08	0.00
C	0.39	0.00	99.61
Co	100.00	0.00	0.00
Cu	100.00	0.00	0.00
Fe	99.96	0.04	0.00
Li	4.64	95.36	0.00
Mn	77.13	22.87	0.00
Ni	100.00	0.00	0.00
Si	60.80	39.20	0.00
O	0.00	27.04	72.96

This paper compares the pyrometallurgical route to the shown hydrometallurgical process route. Fig. 1 summarizes the recycling processes to be compared. As many companies only recycle LIBs to black mass [51], pretreatment is not considered further in the calculation. Additionally, only the first marketable nickel-cobalt products are targeted: the alloy from the pyrometallurgical route and the intermediates from the hydrometallurgical route. Additionally, by-products of both process routes are considered, such as the slag used as a construction material and the other intermediate products generated during the hydrometallurgical processing.

2.2. Total cost of ownership and net present value

The TCO method enables a detailed examination of the total costs associated with owning a good or performing a process [31]. The purchase price is a particular element in the initial consideration of costs [17], especially for capital-intensive industrial processes. However, on closer examination, price is only one component of many that affect the total cost over an asset's lifetime [17,41]. The TCO method, therefore, covers not only procurement and thus the purchase price, but rather the entire life-cycle costs, including maintenance, operation, replacement, disposal, and much more [29,30]. Therefore, the method takes a holistic approach over the entire useful lifetime of the asset under consideration [16,30]. Evaluating the total cost of an asset makes TCO a logical and easy-to-understand approach [31,32]. Because the cost structure is specific to an asset, its use, and its owner, there is no single TCO model, so determining the associated activities and cost-driving factors is the starting point for applying the TCO approach [5,17,41]. Besides all the advantages, one main downside of the TCO method is that it requires detailed accounting and cost data for all cost factors to be considered [30]. Additionally, uncertainties can be introduced regarding cost drivers that are difficult to estimate accurately to account for different possible scenarios over the asset's lifetime [16,46].

As an extension of the TCO method discussed in much of the relevant literature, the TCO model used in this work also includes revenues. Therefore, all cash flows associated with the operation of the recycling processes are considered in the evaluation. The annual TCO is calculated as shown in Eq. (1), where *NPV* is the net present value, T is the total planning horizon, and i is the discount rate.

$$TCO = NPV \frac{(1+i)^T \bullet i}{(1+i)^T - 1} \tag{1}$$

The net present value is obtained from Eq. (2), where C_{Capex} is the initial capital expenditure, $C_{\text{Opex},t}$ is the operating expenditure, and R_t is the revenue in each period t on an annual basis, T is the total planning horizon, and i is the discount rate.

$$NPV = -C_{Capex} + \sum_{t=1}^{T} \frac{R_t - C_{Opex,t}}{(1+i)^t} \tag{2}$$

Since all assets are expected to be used throughout their lifetime and then replaced accordingly, no resale values are included in the calculation as they are assumed to be zero at the end of the period under consideration. It is also assumed that neither buildings nor equipment need to be replaced during this period. Therefore, capital expenditures are incurred only as initial costs and not annually.

3. Theory and calculation

In Section 3.1, the calculation of prices for materials, energy, waste disposal, and CO_2 emissions is described. Subsequently, four price development scenarios are defined to estimate future price developments under uncertainty. Then, the focus is on the currently used LIB types in the LIB market to define three market share scenarios for

Table 2
Distribution coefficients hydrometallurgical recycling process based on own experiments (own table).

Element	Output in %					
	Li_2CO_3	Graphite	Cement Cu	Al/Fe hydroxide	Ni/Co/Mn hydroxide	Residual solution
Al	1.20	5.30	0.00	91.65	1.73	0.13
C	0.00	100.00	0.00	0.00	0.00	0.00
Co	0.00	0.00	0.00	11.38	88.59	0.03
Cu	0.00	0.00	100.00	0.00	0.00	0.00
Fe	2.42	0.00	26.96	70.47	0.06	0.08
Li	66.94	0.00	0.81	4.03	7.48	20.74
Mn	0.00	0.00	0.00	0.60	99.28	0.13
Ni	0.00	0.00	0.00	15.13	84.82	0.04

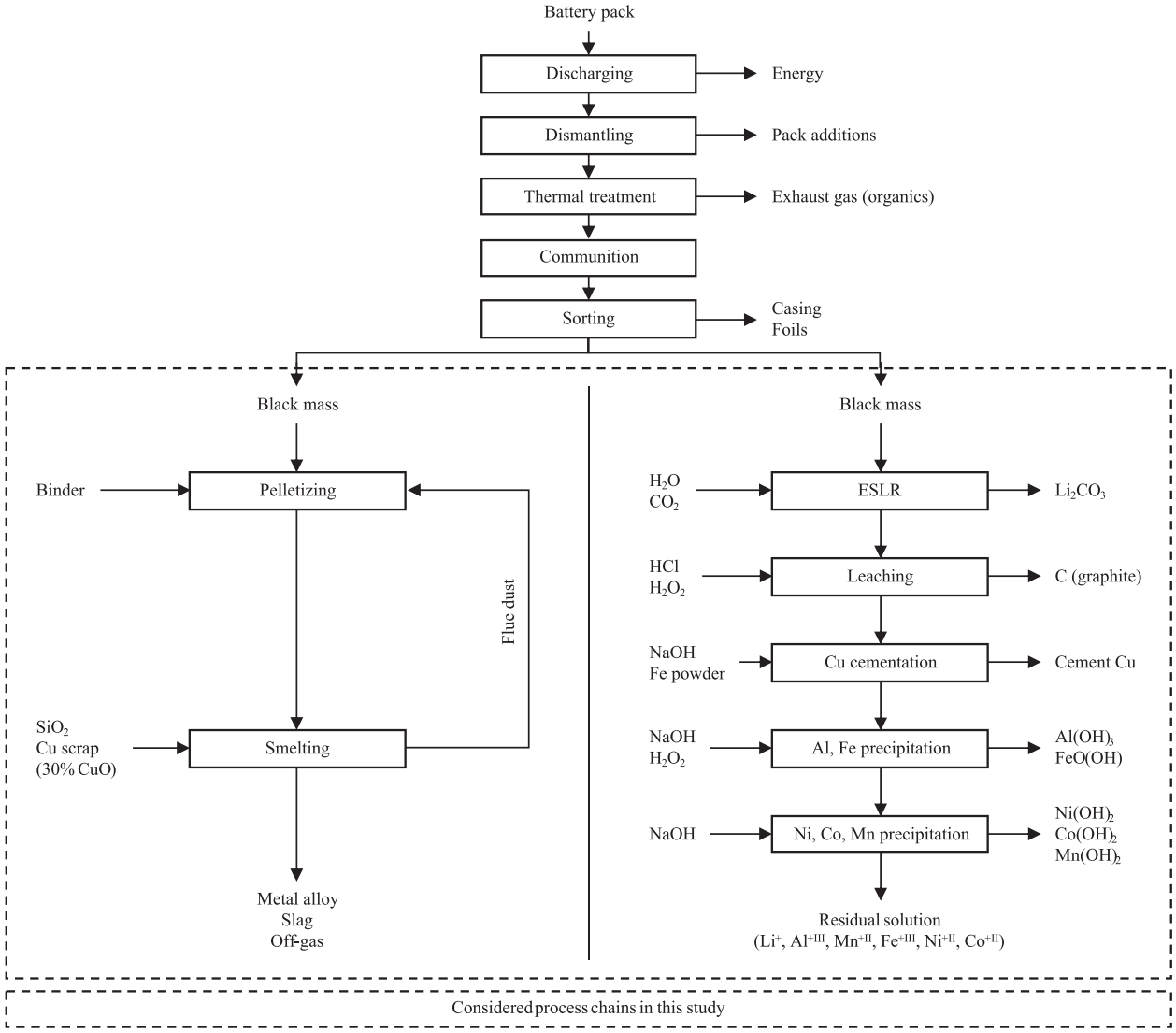

Fig. 1. Process flow charts for pyrometallurgical recycling process (left) and hydrometallurgical recycling process with precedent ESLR (right), adapted from [71,73,84].

possible future developments. Finally, in Section 3.3, the TCO model is set up to evaluate the two recycling processes.

3.1. Material and process auxiliary prices and price development scenarios

Essential parameters for the economic evaluation of recycling processes for LIBs are prices of materials. To enable a cash flow assessment of the material flows, it is necessary to estimate the value of the respective goods and process aids as accurately as possible. Therefore, the goods involved are broken down into units for which prices are available. Section 2.1 overviewed process inputs, outputs, and required process chemicals. In the following, selling prices for the outputs are estimated by breaking down the outputs into their basic components, such as metals and compounds, with respective mass fractions α_i, and then adding the prices for the pure substances proportionally. To account for the lower value due to the blending of the pure substances in the outputs, a markdown of 50% was applied to the respective prices,

which resulted from a discussion with experts. The price estimates for pure substances, as well as price estimates for process chemicals, are derived from exchange prices and available statistics. Energy, water, and disposal costs are estimated based on utility data and statistics. Own experience was used in the few cases where price data were unavailable. Correlations and causalities between price developments of different goods were not considered in detail but may be implicit in the data.

To account for different possible developments in the future, four price scenarios are defined instead of a single price point. For this purpose, a starting price p_j, including a standard deviation $\sigma_{p,j}$, is determined for each material. Based on this, annual growth rates $g_{\mu,j}$ for the mean price and $g_{\sigma,j}$ for the respective standard deviations are estimated using ordinary least squares (OLS) regression. The four price development scenarios represent a fixed, a lower, a base, and an upper case.

Whenever no or insufficient data are available for calculations, predefined default values are used. There is no price growth in the lower scenario, and annual price growth rates are 1.635% and 2.811% for the base and the upper scenario, corresponding to 50% or 100% price growth over 25 years, respectively. In the fixed scenario, the price growth rate is always zero. The default relative standard deviation's starting value is set at 5%. Since the uncertainty of the price forecast increases with a longer time lag, a general annual growth rate for the relative standard deviation of 4% is applied equally to all scenarios. The growth rate was not chosen higher than 4% to keep the probability of negative prices low due to a strongly increased standard deviation. In cases where sufficient data are available for calculations, annual price growth rates are determined and then added to the default values. In this case, the relative standard deviation of prices is calculated based on price data only.

To avoid negative prices in the long term and as a safe side estimate, negative price growth rates were set to zero. This only concerns the price growth rate of HCl in the lower price development scenario (actually −0.01380). On the other hand, individual cases of high price growth rates above 10% were limited to 10% in the upper price development scenario and thus to 7.189% and 8.824% in the lower and base scenarios, respectively, according to the levels of the default growth rates. The cap affects the price growth rates in the lower, base, and upper price development scenarios of cobalt (actually 0.07932, 0.09567, and 0.10743), of Li_2CO_3 (actually 0.10510, and 0.11686), and of CO_2 emission (actually 0.28242, 0.29877, and 0.31053). This approach can be justified by the fact that the prices of the corresponding goods have shown a sharp increase in the recent past, which will most likely not continue in this form in the long term or has already returned to normal [19,20]. The corresponding regressions are, therefore, biased. Limiting the growth rates for prices upward thus serves to limit the bias in the overall result. Detailed prices and parameters of the price development scenario analysis for all materials and process chemicals are shown in Table 3. Since the price increase rates for the fixed scenario are always zero, they have not been included in the table for readability.

Weekly prices for cobalt, copper, and nickel (06/2012 to 12/2022), as well as graphite (10/2017 to 12/2022) are available from commodity exchanges [72]. In a first step, the price data are averaged on an annual basis. The average price of 2022 forms the starting price for further calculations. The starting value for the relative standard deviation is calculated from the data of 2022. A log-linear OLS regression of the average prices on the time dimension yields the annual price growth rates.

Electricity costs are derived from Eurostat data for 2007 to 2022, with energy consumption of between two and 20 GWh per year serving as the basis for pricing [40]. The electricity price is thus 242.70 €/MWh. Water costs are estimated at 2.07 €/m^3 for consumption between 2,001 m^3 and 5,000 m^3 per year [78]. Prices for CuO-containing (30%) scrap, Al/Fe hydroxide disposal, and wastewater treatment, as well as revenue from slag sales, are based on own experience.

All other price data, with the exception of those for CO_2 emissions, are taken from the German foreign trade balance, which provides data sorted by categories [21]. Prices there are not reported on an average basis but on a monthly transaction basis. For each month, total weight and total value are recorded. To obtain average prices per weight unit, a linear OLS regression of transaction values on transaction weights is performed for each month from 01/2006 to 12/2022. The average price of 2022 is set as the starting price for further consideration. A log-linear OLS regression of the prices from the first regression is performed on the time dimension to obtain the annual price growth rates. The starting value for the relative standard deviation is set to default for all prices determined from the German foreign trade balance.

As part of the EU Emissions Trading System (EU-ETS), European legislation provides for the purchase of CO_2 certificates to compensate for greenhouse gas emissions [34,36]. In the cap-and-trade system, one allowance is required for each ton of CO_2 equivalent emitted. Even though some allowances are actually allocated free of charge as part of the grandfathering mechanism [37], costs are calculated for each ton of CO_2 emissions in the sensitivity analysis. Certificate price data are available from the European Energy Exchange [28] on a weekly basis from 05/2021 to 12/2022 and are treated like commodity exchange data described above. The German National Emissions Trading Scheme (nEHS) based on the Fuel Emissions Trading Act (BEHG) has no direct impact on costs but may have indirect effects, as it does not target the emitter of greenhouse gases like the EU-ETS, but rather the distributors of fuel [18].

3.2. Common LIB types and market share scenarios

In addition to prices, the cell chemistry of end-of-life LIBs entering the recycling process is an important determinant in the economic evaluation, as more valuable materials such as cobalt in the output increase achievable revenue. Therefore, in this section, typical cell chemistries of current LIBs are reviewed and then combined into three market share scenarios, the impact of which on the profitability of the recycling processes is analyzed later in this paper. Batteries used in the transportation sector, namely in electric vehicles, account for the largest market share compared to stationary applications and consumer electronics [76]. Additionally, more market studies are available estimating the market share of different cell chemistries used in electric vehicles. Therefore, the market share scenarios in this work are based on literature concerning the electric vehicle market.

Table 4 gives an overview of five common cathode compositions of LIBs. Technical characteristics, as well as advantages and disadvantages of different LIB types, are not discussed in this paper, as there are already many articles on this topic like [8,27,50,61] and many more.

Starting with LCO batteries, the electric vehicle battery market has evolved through NCA and NMC111 types to NMC532 and NMC622 and is expected to reach high nickel battery types such as NMC811 in the near future [27,50,63]. Schmuch et al. [69] refer to NCA, NMC532, and NMC622 as "state-of-the-art cathode materials". The general trend is to reduce the cobalt content and increase the nickel content of LIBs. This is partly because cobalt is an expensive metal but also because supply risks for cobalt are expected in the near future [11,56]. Of the LIB types currently in use, LFP is not included in the market share scenarios because it is more commonly used in China [3], and, more importantly, its different cell chemistry makes it less suitable for the recycling processes considered in this work.

Following various studies and forecasts on the market shares of cathode material compositions currently used in LIBs [3,12,75,80], three market share scenarios are defined and presented in Table 5. The scenarios differ in how quickly batteries with high cobalt content are replaced by batteries with high nickel content in the market. Only graphite is assumed to be the anode active material, as this anode type currently has the highest market share [12,69]. However, anode composition is also evolving towards graphite silicon blends [12,63,80].

To be able to calculate the specific material flows for the market

Table 3
Prices and parameters of the price development scenarios (own table).

Material i	Price		Price growth rate			Rel. std. dev.	
	Start value		Lower scenario	Base scenario	Upper scenario	Start value	Growth rate
	p_j		$g_{\mu l,j}$	$g_{\mu b,j}$	$g_{\mu u,j}$	$\sigma_{p,j}$	$g_{\sigma,j}$
Cobalt	60,168.64	€/t	0.07189	0.08824	0.10000	0.22215	0.04
Copper	9,523.46	€/t	0.03366	0.05001	0.06177	0.07363	0.04
Nickel	28,164.14	€/t	0.05217	0.06852	0.08028	0.11526	0.04
Graphite	3,134.36	€/t	0.05120	0.06755	0.07931	0.07752	0.04
$Co(OH)_2$	31,472.58	€/t	0.00027	0.01662	0.02838	0.05000	0.04
$Mn(OH)_2$	4,445.80	€/t	0.00569	0.02204	0.03380	0.05000	0.04
$Ni(OH)_2$	24,674.23	€/t	0.00667	0.02302	0.03478	0.05000	0.04
Li_2CO_3	15,530.68	€/t	0.07189	0.08824	0.10000	0.05000	0.04
CuO (30%) scrap*	300.00	€/t	0.00000	0.01635	0.02811	0.05000	0.04
SiO_2	2,343.19	€/t	0.00352	0.01987	0.03163	0.05000	0.04
HCl	113.63	€/t	0.00000	0.00255	0.01431	0.05000	0.04
H_2O_2	957.07	€/t	0.02911	0.04546	0.05722	0.05000	0.04
Fe powder	3,230.71	€/t	0.03058	0.04693	0.05869	0.05000	0.04
NaOH	1,440.37	€/t	0.05217	0.06852	0.08028	0.05000	0.04
CO_2 (raw material)	205.80	€/t	0.01752	0.03387	0.04563	0.05000	0.04
Water	2.07	€/m^3	0.00000	0.01635	0.02811	0.05000	0.04
Slag (revenue)*	10.00	€/t	0.00000	0.01635	0.02811	0.05000	0.04
Al/Fe hydroxide disposal*	50.00	€/t	0.00000	0.01635	0.02811	0.05000	0.04
Wastewater treatment*	50,000.00	€/year	0.00000	0.01635	0.02811	0.05000	0.04
Electricity	242.70	€/MWh	0.03455	0.05090	0.06266	0.05000	0.04
CO_2 emission	80.83	€/t	0.07189	0.08824	0.10000	0.08978	0.04

*) Estimates based on own experience.

Table 4
LIB cathode types, adapted from [27,50,61].

LIB type	Formula	Structure
LCO	$LiCoO_2$	Layered
LMO	$LiMn_2O_4$	Spinel
LFP	$LiFePO_4$	Olivine
NCA	$LiNi_{0.8}Co_{0.15}Al_{0.05}O_2$	Layered
NMC	$LiNi_xMn_yCo_zO_2$ (with $x+y+z=1$)	Layered
e.g., NMC532	$LiNi_{0.5}Mn_{0.3}Co_{0.2}O_2$	Layered

Table 5
Definition of market share scenarios (own table).

LIB type	Market share depending on scenario		
	Lower scenario	Base scenario	Upper scenario
LMO	0.05	0.00	0.00
NCA	0.30	0.20	0.10
NMC111	0.20	0.00	0.00
NMC622	0.45	0.60	0.40
NMC811	0.00	0.20	0.50
Sum	1.00	1.00	1.00

share scenarios in both recycling processes considered in this work, ideal-typical black mass compositions for the basic types of LIB cell chemistry are derived based on one average LIB cell component composition defined by Arnberger et al. [2]. According to Arnberger et al. [2], an average LIB cell consists of 31.5% cathode and 18.0% anode active mass, 15.8% cell casing, 6.2% cathode and 10.6% anode current collector foils, 11.6% electrolyte, and 6.2% separator. The LIB cells are assumed to undergo thermal and mechanical pretreatment, as mentioned in Section 2.1, resulting in a BM fraction composed of the anode and cathode active materials that are contaminated by cell housing and current collector foil residues. Complete removal of the electrolyte, binder, and separator material through thermal treatment is assumed in this work for simplification purposes. Therefore, this work does not consider fluorine, phosphorus, and organic compounds. Accurec Recycling GmbH [1] reported that cell components contribute to an overall recycling efficiency of 65.2% for combined thermal and multistep mechanical pretreatment. Based on the contribution to the recycling efficiency per component and their corresponding input mass fractions, percentage recovery rates per component for the Accurec process are derived. The calculations show that 86.0% of steel, which is considered pure iron, and 94.1% of copper foils can be recovered as metal scrap fractions, resulting in a share of 14.0% iron and 5.9% copper of a LIB cell contaminating the BM fraction. The BM contamination by aluminum cannot be calculated based on recycling efficiency due to the loss of most aluminum in the non-ferrous fraction during mechanical treatment. Therefore, a share of 15.0% aluminum foil fraction is assumed to end in the BM fraction. For NMC containing BM, this results in an aluminum content of around 2.0%, which is consistent with the material characterizations presented by Stallmeister et al. [74]. Regarding the active material, 78.7% of graphite, 95.9% of cobalt, and 97.0% of nickel are present in the black mass fraction. No data is available regarding the lithium, manganese, and cathode aluminum of NCA cells. Therefore, the same share as nickel is chosen since this indicates the share of active material ending up in the black mass fraction. Based on the average cell component composition and recovery rates per element, the ideal-typical black mass compositions for basic LIB cell chemistry types are presented in Table 6.

3.3. TCO model for LIB recycling processes

This paper's calculations on recycling processes are based on a holistic TCO model that includes revenues from recycling products. The structure of the TCO model is shown in Fig. 2.

The capital expenditures consist of initial investments in buildings C_B and plants C_P. Investment costs include delivery and installation fees based on previous studies and offers. The planned facilities are designed for pre-industrial scale capacities of 50 kg/h for both the pyrometallurgical and hydrometallurgical recycling routes. Based on experience, a service life of 25 years is assumed for all relevant equipment without the need for replacement during this period. Excluding buildings and equipment not directly related to the pyrometallurgical or hydrometallurgical process, capital expenditures C_{Capex} amount to approximately 7 million € for the pyrometallurgical and 7.5 million € for the

Table 6
Ideal-typical black mass compositions for basic types of LIB cell chemistry (own table).

LIB type	Element mass fraction of black mass in wt%								
	Al	C	Co	Cu	Fe	Li	Mn	Ni	O
LMO	1.918	29.215	0.000	1.294	4.556	2.419	38.294	0.000	22.304
NCA	11.208	29.285	20.042	1.297	4.567	2.388	0.000	20.199	11.012
NMC111	1.921	29.260	12.701	1.296	4.563	4.541	11.982	12.801	20.936
NMC422	1.920	29.245	8.625	1.296	4.561	5.139	8.136	17.385	23.694
NMC532	1.919	29.242	7.609	1.295	4.560	4.534	10.767	19.171	20.903
NMC622	1.919	29.242	7.579	1.295	4.560	4.516	7.150	22.916	20.822
NMC811	1.919	29.228	3.774	1.295	4.558	4.498	3.560	30.430	20.737
NMC9.5.5	1.918	29.222	1.883	1.295	4.557	4.489	1.777	34.165	20.695

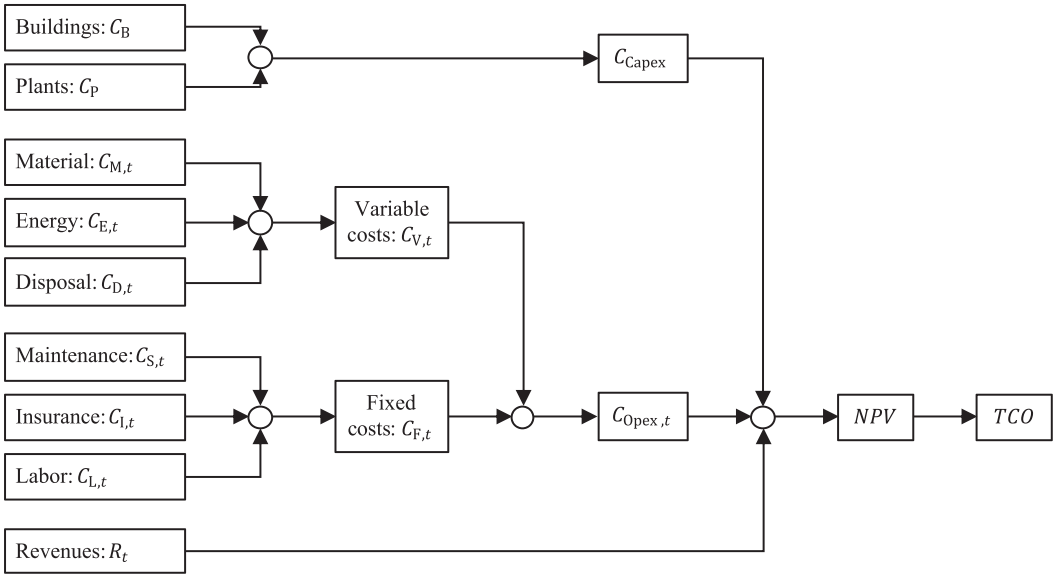

Fig. 2. TCO model (own figure).

hydrometallurgical process. The share of plant investments in this total is 73% for the pyrometallurgical process and 53% for the hydrometallurgical process. Upfront capital expenditures for plants include general equipment like cranes and safety equipment, including off-gas and wastewater treatment, if required. Besides, the main component for the pyrometallurgical process is the furnace, including auxiliary equipment such as ladles, while the plants for the hydrometallurgical process mainly consist of leaching tanks and dosage systems. The costs of the individual system components have been determined based on indicative price quotations obtained or, in some cases, based on experience. Investments in required building space account for 27% of the capex position for the pyrometallurgical process route and 47% for the hydrometallurgical process route. The investment costs for the buildings were calculated by using the costs of institute and laboratory buildings given by the BKI [6] as a guide.

The annual operating expenditures $C_{Opex,t}$ consist of both fixed and variable costs. Fixed costs $C_{F,t}$ are incurred for maintenance $C_{S,t}$, insurance $C_{I,t}$, and labor $C_{L,t}$. Maintenance and insurance costs depend on the investment costs of buildings and plants. They are calculated on a percentage basis. The corresponding markup factors were taken from Bärwaldt and Kwade [4], adjusted based on expert advice, and are listed in Table 7.

Labor costs are expenses for employees. In Germany, employer personal costs comprise gross wages and employer contributions to social security and insurance costs. Gross wages are estimated at 3,156 € per employee and month based on wage groups EG8/9 [54]. Contributions to social security include half of each 2.6% for unemployment insurance[1], 3.05% for long-term care insurance[2], 18.6% for pension insurance[3], and 14.6%[4] plus 1.3% for health insurance [9]. The amount of accident insurance depends on various parameters[5] and is set here at 1%. The markups for the employer's social security contributions and the insurance costs thus add up to 21.075%. Since a three-shift operation with shifts of eight hours each is planned, surcharges of 15% for late shifts and 25% for night shifts on the gross wage have to be considered [55]. Finally, an annual surcharge of approximately 70% of the gross monthly wage is due as part of the vacation pay [53]. Overall, average

Table 7
Markup factors for maintenance and insurance (own table).

Category	Markup factor in %
Maintenance costs	
Buildings	1.50
Plants	3.00
Insurance costs	
Buildings	1.00
Plants	1.00

[1] See § 341(2) SGB III in [25].
[2] See § 55(1) SGB XI in [23].
[3] See § 1 BSV 2018 in [13].
[4] See § 241 SGB V in [22].
[5] See § 153(1) SGB VII in [24].

labor costs are estimated at 56,000 € per employee and year. For the processes considered in this paper, an average requirement of three employees per shift is assumed for the pyrometallurgical process and 1.5 employees per shift for the hydrometallurgical process. The labor costs for 250 working days per year thus amount to 504,000 € for the pyrometallurgical process and 252,000 € for the hydrometallurgical process.

Variable costs $C_{V,t}$ include expenses for material $C_{M,t}$, energy $C_{E,t}$, and waste disposal $C_{D,t}$. Respective prices were derived in Section 3.1. According to material flows in both recycling routes in the three market share scenarios for LIB types and the four price development scenarios, the aggregated material prices can be calculated using Eq. (3) and Eq. (4), where j indexes the set of pure substances contained in each output and α_j is the respective mass fraction of a pure substance j. As described in Section 3.1, a markdown of 50% (see Eq. (3)) was applied for the first calculations. From this, the total material costs can be derived. Expenses for the procurement of pyrolyzed black mass are not included in the cost of materials at this point. The calculated TCO per ton of recycled black mass can, therefore, be interpreted as the maximum price per ton of black mass to be recycled in purchasing or internal transfer price. If this price is exceeded, the process is not profitable from a financial point of view. The same procedure results in total waste disposal costs. Knowing the total installed power and utilization rate of each plant, in combination with the electricity price, leads to the total energy costs. Since the general energy consumption is low compared to the process energy consumption, it is neglected in the calculations. For all processes, the actual uptime factor is set to 95%. In the remaining 5%, fixed costs and energy costs accrue, but no material passes through production. Handling costs are assumed to be covered by the other cost categories.

$$p_t = 0.5\sum_j \alpha_j p_j \left(1 + g_{\mu,j}\right)^t \tag{3}$$

$$\sigma_{p,t} = \sqrt{\sum_j \left(\alpha_j \sigma_{p,j} \left(1 + g_{\sigma,j}\right)^t\right)^2} \tag{4}$$

The general determinants of the TCO model are the observation period T and the discount rate i. If both the beta factor and the debt-equity ratio of the fictitious company carrying out the recycling processes are constant over time and match the corresponding values of the sector, the weighted average cost of capital (WACC) of the sector can be used as the discount rate.[6] The WACC sector value for the materials industry was 8.1% in December 2022 [66]. The period under consideration is set at 25 years. In general, all values are calculated, taking uncertainty into account. Therefore, a standard deviation is given in addition to each mean value.

4. Results and discussion

The following section presents the results of the TCO calculations based on the model and data developed in Section 3. This includes a discussion of the impact of the different scenarios for market share development of the chemical composition of LIB cells and for the price development on the economic feasibility of the two recycling process routes introduced in Section 2.1. Sensitivity analyses are then used to assess uncertainties in the results. The material and energy flows considered for both recycling approaches are provided in Appendix B.

4.1. TCO of the pyrometallurgical recycling route

With a forecast horizon of 25 years and a pyrometallurgical processing of 285 t of pyrolyzed black mass (BM) per year, the economic picture is mixed. The results for the pyrometallurgical recycling route for all previously mentioned scenarios are shown in Table 8. It should be noted that results do not account for the expenses of generating the black mass to be recycled, as described in Section 3.3. Therefore, the TCO per ton of recycled black mass presented here can be understood as the maximum purchase price for black mass until the process becomes unprofitable.

At first glance, two general trends are immediately apparent: First, the economic feasibility of the pyrometallurgical recycling process develops positively from the fixed to the upper price development scenario. Second, the economic feasibility develops negatively from the lower to the upper market scenario. The first trend can be explained by stronger increasing product prices compared to raw material costs. Taking a closer look at the results of the calculations, the revenues from the sale of the metal alloy exceed those of the slag by far (factor 2,275 to 6,377, depending on the scenario). This is because most valuable materials, such as cobalt, nickel, and copper, are contained in the alloy, while the lower-value materials are found in the slag. Among other things, the slag is often used only in the construction industry and is therefore of little value, as mentioned earlier. Nevertheless, almost all the lithium is contained in the slag. However, the valuable lithium is unfavorably bound and would have to be separated from the other slag components by subsequent recycling processes to represent a valuable process output. This leads to the second overarching trend. Since there are only two very aggregate process outputs in the pyrometallurgical process, value is created not so much by breaking down the pyrolyzed black mass into pure materials but by concentrating more valuable materials in one output, the alloy. Therefore, pyrometallurgy is very sensitive to the content of high-value metals in the black mass. While the mass fraction of cobalt in the black mass decreases from 11.964% in the lower market scenario to 6.923% in the upper market scenario, the value of the alloy reduces accordingly. An increase in the nickel content of the black mass from 18.932% to 26.402% over the same scenarios cannot compensate for the loss in value. Especially for the TCO values close to

Table 8
TCO and NPV of the pyrometallurgical recycling route for all market and price development scenarios with standard deviations in brackets (own table).

Price scenario		Market scenario		
		Lower	Base	Upper
Fixed	TCO total	−199,730.98 € (41,728.83 €)	−505,417.50 € (35,843.57 €)	−721,367.50 € (31,530.45 €)
	TCO / t BM	−700.81 € (146.42 €)	−1,773.39 € (125.77 €)	−2,531.11 € (110.63 €)
	NPV	−2,113,996.60 € (441,667.12 €)	−5,349,449.85 € (379,376.21 €)	−7,635,112.08 € (333,725.16 €)
Lower	TCO total	1,036,722.62 € (75,799.44 €)	460,962.87 € (63,305.44 €)	38,018.29 € (53,770.03 €)
	TCO / t BM	3,637.62 € (265.96 €)	1,617.41 € (222,12 €)	133,40 € (188.67 €)
	NPV	10,972,899.93 € (802,277.97 €)	4,878,932.25 € (670,038.68 €)	402,393.95 € (569,113.85 €)
Base	TCO total	1,523,574.14 € (94,719.90 €)	835,308.40 € (78,910.83 €)	328,712.18 € (66,801.82 €)
	TCO / t BM	5,345.87 € (332.35 €)	2,930.91 € (276.88 €)	1,153.38 € (234.39 €)
	NPV	16,125,843.33 € (1,002,536.20 €)	8,841,087.59 € (835,209.59 €)	3,479,161.87 € (707,045.11 €)
Upper	TCO total	1,951,087.27 € (112,431.18 €)	1,164,123.65 € (93,552.98 €)	584,089.25 € (79,008.03 €)
	TCO / t BM	6,845.92 € (394.50 €)	4,084.64 € (328.15 €)	2,049.44 € (277.22 €)
	NPV	20,650,736.24 € (1,189,996.28 €)	12,321,340.40 € (989,867.78 €)	6,182,128.95 € (836,238.39 €)

[6] This is because, according to the capital asset pricing model, $r_i = r_f + (r_m - r_f)\beta_{i,m}$ with the return r_i of the capital asset i, the risk-free interest rate r_f, and the return r_m of the market portfolio. Thus, if $\beta_{company,m} = \beta_{sector,m}$, then $r_{company} = r_{sector}$.

zero in Table 8, there are relatively high standard deviations compared to the given mean. This is due to the way the values are calculated, as in these cases the cash inflows and outflows almost cancel each other out when calculating the mean value, which is not the case for the corresponding standard deviations.

The pyrometallurgical recycling process is relatively energy-intensive due to using an electronic arc furnace. Energy costs account for 45.3% of operating costs on average in the base market and base price scenario (baseline scenario) and represent the most significant cost factor. The second most important cost factor is labor at 23.3%, directly followed by material costs, which add up to 19.6% of operating expenses in the same scenario. Looking at the process parameters and scale, the pyrometallurgical process technically requires continuous operation so that the furnace does not have to be reheated regularly. This requirement is partially met here by the three-shift operation. However, the operation should be guaranteed not only for 250 working days but also continuously. Fixed costs are high relative to the variable costs (34.9% vs. 65.1% in the baseline scenario). Thus, an increase in throughput could improve the fixed costs share but also the investment costs in relation to the throughput items.

4.2. TCO of the hydrometallurgical recycling route

For the hydrometallurgical recycling process over a 25-year analysis period, processing 285 t of pyrolyzed black mass per year, positive TCO is achieved in every scenario. Again, the costs of generating the black mass to be recycled are not included in the calculations, so the results can again be interpreted as described above. The results for the hydrometallurgical recycling route for all market and price scenarios are shown in Table 9.

The hydrometallurgical recycling process shows the same trend as the pyrometallurgical route concerning the price scenarios. Thus, the economic feasibility of the hydrometallurgical route develops positively from the fixed to the upper-price development scenario. The detailed calculation tables show that the trend in the price scenarios is due to stronger revenue growth than material costs. Considering the effects along the different market scenarios, the trend of economic feasibility shows a positive development from the lower to the upper market scenario. However, the results of the market scenarios, especially between the base and upper scenario, only differ slightly. The hydrometallurgical recycling route yields five output fractions, some with highly concentrated pure substances. This leads to high values of these products, as the purity allows direct reuse of the materials also in battery production. The difference in prices and price growth rates of $Co(OH)_2$ and $Ni(OH)_2$ is smaller than between cobalt and nickel as metals. The decrease of cobalt in the black mass from 11.964% in the lower market scenario to 6.923% in the upper market scenario can be partly compensated by the higher increase of nickel from 18.932% to 26.402% over the same scenarios. The almost continuous decline in black mass cobalt content across the three market scenarios, combined with a 4.9 percentage point increase in nickel content from the lower to the base market scenario and a 2.5 percentage point increase from the base to the upper market scenario, explains the trend in profitability across the market scenarios.

Due to the pre-industrial scale of only 50 kg/h pyrolyzed black mass processed in the hydrometallurgical recycling route, average fixed costs, about half of which are labor costs, account for 23.3% of the operation expenditures in the base market and base price scenario, for example. Higher material throughput by upscaling should lower the share of fixed costs and thus further increase the profitability of the hydrometallurgical recycling route. Several process chemicals are used in hydrometallurgy, so the material costs for these process inputs are quite high, averaging 41.4% in the baseline scenario. Energy costs average 32.2% of operating expenditures in the baseline scenario. In particular, the energy consumption of the ESLR process due to high process temperature and pressure could be reduced in the future by adjusting the process parameters, according to Schwich et al. [71].

Table 9
TCO and NPV of the hydrometallurgical recycling route for all market and price development scenarios with standard deviations in brackets (own table).

Price scenario		Market scenario		
		Lower	Base	Upper
Fixed	TCO total	427,582.81 € (19,015.72 €)	517,499.06 € (21,033.15 €)	516,196.74 € (21,909.94 €)
	TCO / t BM	1,500.29 € (66.72 €)	1,815.79 € (73.80 €)	1,811.22 € (76.88 €)
	NPV	4,525,630.39 € (201,266.50 €)	5,477,323.66 € (222,619.46 €)	5,463,539.66 € (231,899.64 €)
Lower	TCO total	832,417.96 € (27,569.74 €)	981,617.22 € (30,040.88 €)	1,018,521.96 € (31,361.29 €)
	TCO / t BM	2,920.76 € (96.74 €)	3,444.27 € (105.41 €)	3,573,76 € (110,04 €)
	NPV	8,810,494.56 € (291,804.14 €)	10,389,652.29 € (317,959.23 €)	10,780,260.18 € (331,934.80 €)
Base	TCO total	1,183,421.52 € (33,877.84 €)	1,360,566.62 € (36,853.38 €)	1,406,695.02 € (38,481.60 €)
	TCO / t BM	4,152.36 € (118.87 €)	4,773.92 € (129.31 €)	4,935.77 € (135.02 €)
	NPV	12,525.593.28 € (358,570.52 €)	14,400,535.89 € (390,064.30 €)	14,888,769.04 € (407,297.69 €)
Upper	TCO total	1,484.527.52 € (39,803.45 €)	1,686,124.29 € (43,253.61 €)	1,740,446.64 € (45,170.69 €)
	TCO / t BM	5,208.87 € (139.66 €)	5,916.23 € (151.77 €)	6,106.83 € (158.49 €)
	NPV	15,712,565.31 € (421,288.49 €)	17,846,309.83 € (457,805.73 €)	18,421,269.54 € (478,096.49 €)

4.3. Sensitivity analysis

To account for uncertainties in the results presented in Sections 4.1 and 4.2, the effects of important parameters of the calculations on the results are evaluated in sensitivity analyses. Energy and material costs account for a large share of operating expenditures in both recycling routes. Therefore, the impact of variations in electricity price and price markdowns on marketable process outputs are examined first.

Considering a variation of the start price for electricity of 242.70 €/MWh between −100% and 100%, it follows that the slope of TCO per ton of processed pyrolyzed black mass is consistently negative and steepest for the upper price development scenarios (−32.07 €/pp. and − 22.48 €/pp) and flattest for the fixed price development scenarios (−17.89 €/pp. and − 12.54 €/pp) for both the pyrometallurgical and the hydrometallurgical recycling process. On average, the slope is −25.56 €/pp. for the pyrometallurgical and − 17.99 €/pp. for the hydrometallurgical recycling process. Relative to the value without variation (see Fig. 3), the average slope is −2.616%/pp. (min: −0.468%/pp., max: −18.175%/pp) for the pyrometallurgical recycling process and − 0.521%/pp. (min: −0.368%/pp., max: −0.836%/pp) for the hydrometallurgical recycling process. Differentiating the start price for electricity between −100% and 100% does not lead to any changes in the sign regarding economic feasibility for the hydrometallurgical process. Regarding the pyrometallurgical process, there are changes in six scenarios. The respective break-even points are reported in Table 10.

This analysis shows that the results for the pyrometallurgical process are significantly more sensitive to a variation in electricity price than the results for the hydrometallurgical process. This can also be seen in Fig. 3 and is due to the share of energy costs in the operating expenditures. For the hydrometallurgical recycling process, the initial values of the TCO per ton of pyrolyzed black mass processed are sufficiently high that even doubling the start electricity price does not lead to a negative TCO in any scenario. Detailed charts showing the impact of the electricity base price on TCO are provided in Appendix C.

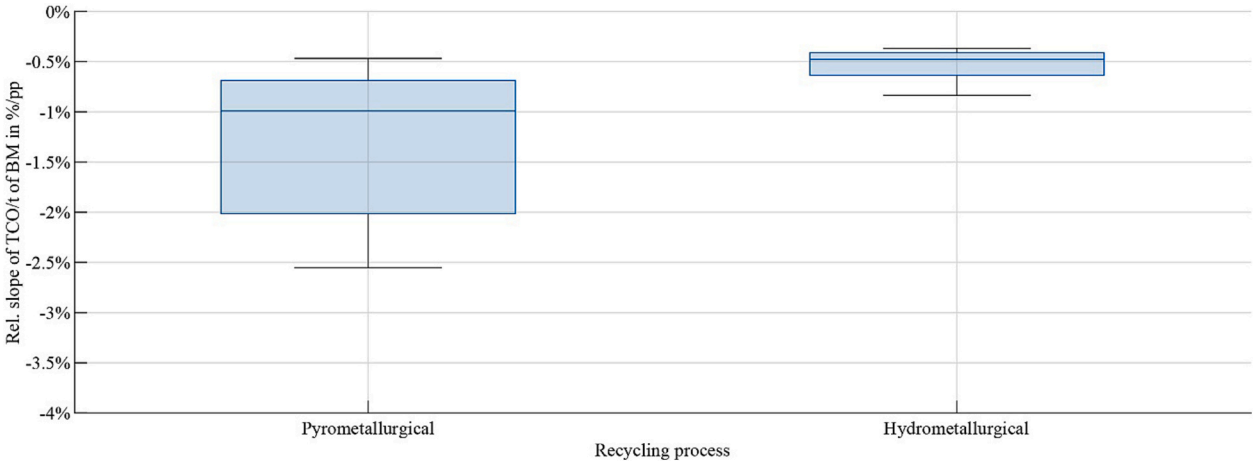

Fig. 3. Relative slopes of TCO per t of BM processed with varying electricity base price for all scenarios of both recycling routes, not showing the outlier at −18.175% for the pyrometallurgical process for clarity (own figure).

Table 10
Break-even points in energy price sensitivity analysis for the pyrometallurgical process (own table).

Market scenario	Price scenario	Break-even point
Lower	Fixed	−39.18%
Base	Fixed	−99.15%
Base	Lower	66.71%
Upper	Lower	5.50%
Upper	Base	40.57%
Upper	Upper	63.91%

The price markdown on marketable process outputs can vary from 0% if the process output would be prorated at the market price for the respective pure materials to 100% if the process output would be valued as worthless. The slope of the TCO per ton of processed black mass with varying markdown is negative for all scenarios in both recycling processes. This is plausible since a higher markdown leads to a lower selling price for the respective process output and thus to a lower overall revenue. Table 11 gives an overview of the absolute slopes of the TCO per ton of processed black mass related to the variation in the price markdown on the process outputs, as well as the relative slopes where the absolute slope is related to the initial value of the TCO, which results at the 50% price markdown defined in Section 3.1.

From the values presented in Table 11 and the graphs shown in Fig. 4, it is evident that the pyrometallurgical recycling process is more sensitive to higher price markdowns on marketable process outputs than the hydrometallurgical recycling process. Within the hydrometallurgical recycling process, the Ni/Co/Mn hydroxide output fraction is primarily sensitive to price markdowns. The other outputs do not cause as much variation in the TCO per ton of processed black mass with changes in the respective price markdowns. These results are understandable to the extent that they reflect the shares of the respective process outputs in the revenue for the hydrometallurgical recycling process. For the pyrometallurgical recycling process, the alloy represents the only relevant marketable process output. Therefore, it also bears the full variation of the price markdown in relation to the overall result.

Changes in the price markdown between 0% and 100% for Li_2CO_3, graphite, and cement Cu do not lead to a change in the sign of the TCO. For Ni/Co/Mn hydroxide, only the fixed price development scenarios result in break-even points for very high price markdowns of 74.9–79.9%, depending on the market scenario, and the lower price development scenario in combination with the lower market scenario results in a break-even price markdown of 96.9%. Regarding the alloy from the pyrometallurgical recycling process, there is a break-even point for all scenarios. For the remaining scenarios, which have a positive TCO prior to the sensitivity analysis, the discounts for the break-even point are very high at 61.2–91.4%. For the upper market scenario in the lower price development scenario, however, only a slightly increased price markdown of 51.5% would be required for the break-even point. On the other hand, the three scenarios in which the TCO was negative in advance could also be brought to the break-even point with reduced price markdowns of 40.3% for the lower market scenario, 21.2% for the base market scenario, and 3.2% for the higher market scenario. Detailed charts showing the impact of the price markdowns on TCO are provided in Appendix C.

Finally, in this section, the effect of compensating for externalities through the purchase of CO_2 emission allowances on the results is examined. Using the price growth rates presented in Section 3.1, the inclusion of CO_2 emission allowances inherently leads to a reduction in TCO per ton of pyrolyzed black mass processed. The variation in results by market and price growth scenarios is shown in Table 12. Since CO_2 emissions only occur in the pyrometallurgical recycling process, there are no changes to the hydrometallurgical recycling process.

Table 11
Ranges of absolute and relative slopes of TCO per t of BM processed with varying price markdown on marketable process outputs (own table).

Process	Marketable output	Min	Avg.	Std. dev.	Max
Pyrometallurgy	Alloy	−54.06 €/pp	−107.53 €/pp	32.76 €/pp	−165.51 €/pp
		−2.136%/pp	−9.860%/pp	16.922%/pp	−65.372%/pp
Hydrometallurgy	Li_2CO_3	−20.91 €/pp	−45.21 €/pp	14.61 €/pp	−64.51 €/pp
		−1.038%/pp	−1.219%/pp	0.125%/pp	−1.416%/pp
	Graphite	−4.58 €/pp	−7.59 €/pp	1.95 €/pp	−9.83 €/pp
		−0.161%/pp	−0.213%/pp	0.042%/pp	−0.306%/pp
	Cement Cu	−0.62 €/pp	−0.88 €/pp	0.18 €/pp	−1.1 €/pp
		−0.018%/pp	−0.025%/pp	0.007%/pp	−0.041%/pp
	Ni/Co/Mn hydroxide	−60.29 €/pp	−69.44 €/pp	8.07 €/pp	−82.22 €/pp
		−1.326%/pp	−2.126%/pp	0.882%/pp	−4.018%/pp

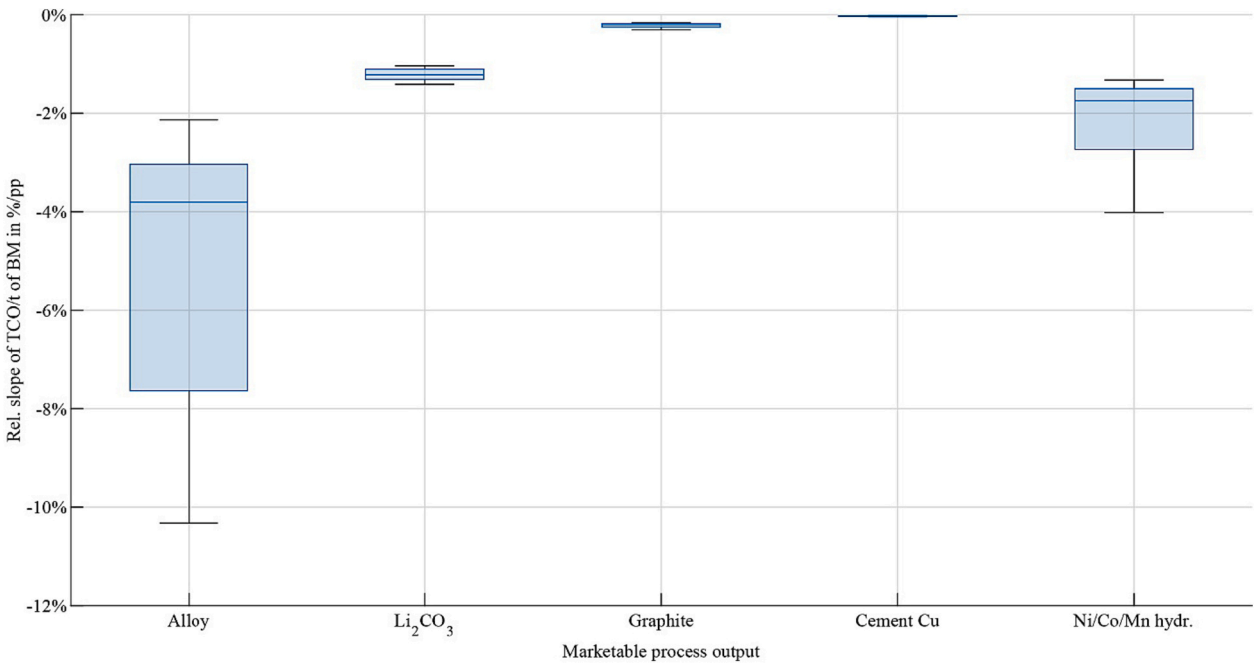

Fig. 4. Relative slopes of TCO per t of BM processed with varying price markdowns on marketable process outputs for all scenarios of both recycling routes, not showing the outlier at −65.372% for alloy for clarity (own figure).

Table 12
Impact of compensating for CO_2 emissions on the TCO per t of BM processed for the pyrometallurgical recycling process (own table).

Price scenario	Market scenario		
	Lower	Base	Upper
Fixed	−86.32 €	−86.29 €	−86.27 €
Lower	−170.71 €	−170.65 €	−170.61 €
Base	−204.57 €	−204.51 €	−204.45 €
Upper	−234.30 €	−234.23 €	−234.16 €

As can be seen, the values for the three market scenarios hardly differ in each case. Since the price of CO_2 certificates will likely continue to rise sharply in the future, and more and more industries will be obliged to compensate for their emissions by purchasing CO_2 certificates, this cost item is certainly relevant for the processes considered here.

4.4. Comparison of both recycling routes and limitations of the economic evaluation

Comparing the results for both recycling routes, the pyrometallurgical recycling route shows higher profitability than the hydrometallurgical route in lower market scenario for the lower to upper price development scenarios. In the other cases, the hydrometallurgical recycling process is economically advantageous. Except for the pyrometallurgical recycling process in the fixed price development scenarios in all market scenarios, both processes have positive TCO in all scenarios. However, it should be noted that the calculations do not include expenses for the production of pyrolyzed black mass. Furthermore, in this study it is assumed that the lithium-bearing slag produced in the pyrometallurgical process is sold to the construction sector as a filler material.

Looking at the development of the TCO per ton of processed black mass over the different scenarios comparing the two recycling routes, the hydrometallurgical recycling route shows more constant results. Furthermore, the respective standard deviation is lower than the corresponding values of the pyrometallurgical recycling route. This implies that the hydrometallurgical recycling route is both less susceptible to price fluctuations and less dependent on the composition of the recycled black mass than the pyrometallurgical recycling route. In particular, a decreasing cobalt content has less impact on the outcome. This can be explained by a more diversified output with fewer and more highly concentrated materials per fraction in the hydrometallurgical recycling route.

Regarding the limitations of the presented evaluations of both recycling processes, the standard deviations to the results presented in Table 8 and Table 9 should be considered first. For the pyrometallurgical recycling route, the standard deviations are quite high compared to the mean values. For the hydrometallurgical route, the ratio is much lower. However, it should be noted that the results are based on assumptions about material prices extending 25 years into the future and may, therefore, differ significantly from actual trends. In particular, the regressions on past prices of cobalt and Li_2CO_3 resulted in high price growth rates in the calculation model. On the one hand, these price increases can be justified by an increasing demand for raw materials in the course of increased battery production [76] combined with a shortage of the corresponding raw materials, as described in Section 1. On the other hand, overly high assumptions regarding price increase rates may also lead to exaggerated expectations regarding revenues for recycled products.

Second, and related to the problem of accurate price forecasting, the price markdowns, which relate the values of recycled products to the pure prices of the substances they contain, have a major impact on the results presented here. There is a high sensitivity of the results with respect to the variation of price markdowns, especially for high-value recycling output fractions. Finally, deviations in the actual market development of LIB cell chemistry also cause variations in the calculation results. However, the general trend of reducing the cobalt content and instead increasing the nickel content of the cathode active material is very likely, as described in Section 3.2.

5. Conclusions

In this paper, two recycling approaches for pyrolyzed black mass from LIBs were evaluated economically. Despite all limitations in the evaluation, general trends were identified on how both recycling routes

perform under different market and price development scenarios. This leads to answering the first research question formulated regarding factors influencing the economic advantageousness of the two recycling processes. The main factors affecting economic feasibility are material and energy prices. Excluding the purchase of pyrolyzed black mass, both recycling processes presented in this paper are profitable in most scenarios – the hydrometallurgical process in all scenarios. The hydrometallurgical recycling route was found to be less susceptible to price fluctuations and changes in cell chemistry than the pyrometallurgical recycling route. Therefore, the hydrometallurgical recycling route is expected to be more profitable than the pyrometallurgical one when scaled up, especially in the context of decreasing cobalt content in LIBs.

Discussion of the chemical composition of LIB cells provides a bridge to answering the second research question regarding future developments that influence the result of the economic evaluation. The most significant changes in the future will be in cell chemistry. As mentioned earlier, the hydrometallurgical process is more robust to specific changes in this regard. However, it is expected that the currently used LIB types will be replaced by more advanced types, such as high-voltage spinel (HVS), high-energy NMC (HE-NMC), solid-state batteries (SSB), lithium-oxygen (LiO_2) batteries, and lithium-sulfur (LiS) batteries, or alternative battery technologies like sodium-ion batteries. For these battery types, the two recycling routes presented in this work are at least partially inapplicable. Therefore, in a market dominated by new LIB types, neither recycling route is likely to be profitable anymore. However, since the market launch of these new LIB types is not yet foreseeable, and there are still large quantities of conventional LIB types in use, both processes have the prospect of profitable operation in the medium term under proper boundary conditions.

To establish and expand suitable collection systems and recycling processes, subsidies should also be considered since raw material recycling, even in the case of processes that are not profitable from a purely economic point of view, can still be advantageous from a macroeconomic point of view when external costs are considered regarding environmental and social impacts.

In further research, the optimization of the recycling efficiency of lithium in the pyrometallurgical recycling route is to be comparatively evaluated. This is technically possible by mobilizing the lithium equally through an upstream ESLR, as in the hydrometallurgical recycling route presented here. Further research could include the integration of pre- and postprocessing steps into the calculations, as well as the consideration of further recycling processes and future battery types. To achieve a more holistic view, external costs related to environmental and social impacts should also be addressed. In addition, more in-depth considerations could be made around collection logistics for end-of-life LIBs.

CRediT authorship contribution statement

Richard Woeste: Writing – original draft, Methodology, Formal analysis. **Emanuel-Sebastian Drude:** Writing – original draft, Methodology, Formal analysis. **Dzeneta Vrucak:** Writing – original draft, Methodology, Formal analysis. **Kai Klöckner:** Formal analysis. **Elinor Rombach:** Writing – review & editing, Project administration, Conceptualization. **Peter Letmathe:** Writing – review & editing, Supervision, Conceptualization. **Bernd Friedrich:** Writing – review & editing, Supervision, Conceptualization.

Declaration of competing interest

The authors declare that they have no known competing financial interests or personal relationships that could have appeared to influence the work reported in this paper.

Data availability

The data that has been used is confidential.

Acknowledgements

This article was written as part of the Recycling & Green Battery (greenBatt) competence cluster. The underlying project was funded by the German Federal Ministry of Education and Research (BMBF) under the funding code 03XP0302. The authors are responsible for the content of this publication.

Appendix A. Experimental description of the hydrometallurgical reference process

A pyrolyzed black mass with a particle size of <1 mm was used as input material for the hydrometallurgical reference process route. The black mass was NMC-based and pre-pyrolyzed. To ensure a low content of residual binder and electrolyte due to a possible insufficient thermal treatment, the black mass powder was first post-pyrolyzed at 600 °C for one hour in a nitrogen atmosphere. To determine the composition of the post-pyrolyzed black mass, a 3 g sample was analyzed using a "Spectro CIROS Vision" inductively coupled plasma-optical emission spectrometer (ICP-OES) manufactured by "SPECTRO Analytical Instruments GmbH, Kleve, Germany". The chemical composition of the output black mass is shown in Table 13.

Table 13
Chemical composition of pyrolyzed black mass used for ESLR and hydrometallurgy in wt% (own table).

Al	Cu	Co	Li	Mn	Ni	Fe	C	F
4.27–5.20	1.85–2.45	11.00	4.30	9.67	13.30	1.11	26.80	–

For the ESLR process step, 150 g of the post-pyrolyzed black mass was leached in water at an S/L ratio of 1:30 for 120 min at 25 °C. CO_2 was injected at a flow rate of 3 l/min, similar to Hu et al. [52] and Yi et al. [86]. After the CO_2-induced water leaching, the suspension of the undissolved black mass residue and the pregnant leaching solution were filtered.

For the subsequent acid leaching, 135 g of the residual black mass was used as initial input material. The experimental parameters for the multistep hydrometallurgical process were based on Wang and Friedrich [85]. The black mass was leached at 80 °C for 120 min with a 4-M hydrochloric acid, a solid/liquid ratio of 1:10, and an addition of 50 g/l hydrogen peroxide. The undissolved graphite residue was then filtered. For the subsequent copper cementation, 1.2 times the amount of copper content was added to the residual solution (the filtrate from the previous process step). Sodium hydroxide pellets (> 99% NaOH, Merck KGaA) were added to adjust the pH to 1.7 at a process temperature of 60 °C, after which the cement copper fraction was filtered. The pH was raised to 3.75 by adding sodium hydroxide pellets at 40 °C and 10 g/l of hydrogen peroxide to precipitate the aluminum/iron hydroxide fraction before filtering. The pH in the remaining filtrate was increased to 10.37 by adding sodium hydroxide pellets before the mixed hydroxide of nickel, manganese, and cobalt was filtered.

For the ESLR process step and each subsequent hydrometallurgical process step, the filter cake was post-washed with a specific amount of water

after filtration to ensure complete separation of all dissolved elements from the filter cake. The volume of each filtrate and the washing solution were measured. To determine the composition of each solution, 3 ml samples were taken. Each sample was diluted in a 1:10 ratio and analyzed via ICP-OES. The element distribution for each process step was determined based on the volumes of the liquid samples and their compositions. As an idealization, it was assumed that the elements dissolved in the washing solution could be added to the filtrate of each process step. From this, the accumulated elemental concentrations of the residual solutions were determined, based on which the elemental distribution for each process step was derived. The accumulated element concentrations of the solution fraction for each hydrometallurgical process step are given in Table 14, while Table 15 displays the element-based distribution coefficients for each process step. Since graphite was not analyzed in this work, it is presumed that 100% will be allocated to the graphite fraction.

Table 14
Accumulated element concentration in the filtrate and washing solution after each process step in g/l (own table).

ESLR						
Al	Cu	Co	Li	Mn	Ni	Fe
0.01	–	–	0.11	–	–	–
Leaching						
Al	Cu	Co	Li	Mn	Ni	Fe
4.17	2.11	10.21	1.25	9.35	12.81	1.14
Copper cementation						
Al	Cu	Co	Li	Mn	Ni	Fe
4.84	–	11.80	1.41	10.85	15.22	2.74
Aluminum and iron precipitation						
Al	Cu	Co	Li	Mn	Ni	Fe
0.13	–	15.07	1.73	15.43	18.48	–
Cobalt, nickel, and manganese precipitation						
Al	Cu	Co	Li	Mn	Ni	Fe
0.01	–	–	1.38	–	–	–

Table 15
Element distribution after each process step in wt% (own table).

ELSR								
	Al	Cu	Co	Li	Mn	Ni	Fe	C
Product	1.20	0.00	0.00	66.94	0.00	0.00	2.42	0.00
Process	98.80	100.00	100.00	33.06	100.00	100.00	97.58	100.00
Leaching								
	Al	Cu	Co	Li	Mn	Ni	Fe	C
Product	5.36	0.00	0.00	0.00	0.00	0.00	0.00	100.00
Process	94.64	100.00	100.00	100.00	100.00	100.00	100.00	0.00
Copper cementation								
	Al	Cu	Co	Li	Mn	Ni	Fe	C
Product	0.00	100.00	0.00	2.45	0.00	0.00	27.63	–
Process	100.00	0.00	100.00	97.55	100.00	100.00	72.37	–
Aluminum and iron precipitation								
	Al	Cu	Co	Li	Mn	Ni	Fe	C
Product	98.01	–	11.38	12.49	0.60	15.13	99.80	–
Process	1.99	–	88.62	87.51	99.40	84.87	0.20	–
Cobalt, nickel, and manganese precipitation								
	Al	Cu	Co	Li	Mn	Ni	Fe	C
Product	93.23	–	99.97	26.50	99.87	99.95	42.01	–
Process	6.77	–	0.03	73.50	0.13	0.05	57.99	–

Appendix B. Material and energy flows of the pyrometallurgical and hydrometallurgical reference process

Based on the determined distribution coefficients from Table 1 and Table 2, and the three defined market share scenarios in Table 5, annual material flows were generated for both recycling approaches. The annual material flows for the lower, base, and upper market share scenario are illustrated in Fig. 5, based on an annual processing of 285 t/a BM.

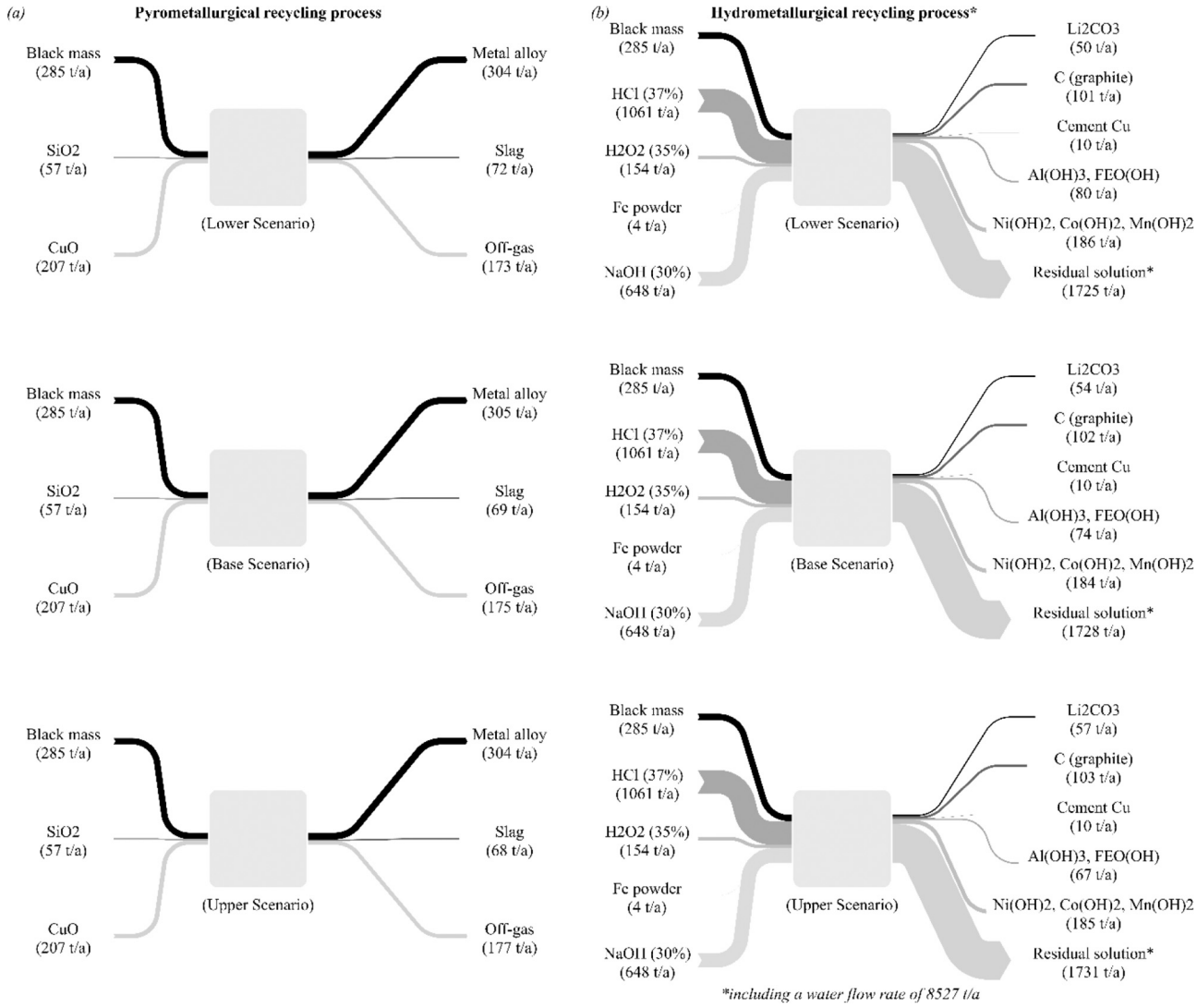

Fig. 5. Annual input and output stream for the lower, base and upper market share scenario for the pyrometallurgical (a) and hydrometallurgical (b) recycling process (own figure).

As a simplifying assumption, the same amount of input materials was considered in each scenario. The differences between the three scenarios arise from the scenario-dependent composition of the BM, which results in different weightings of the output streams.

The annual electricity consumption for both recycling processes was determined based on the rated power of the pre-defined pilot-scale plant technology. For the pyrometallurgical process route, an annual energy consumption of 2,100.3 MWh/a was calculated, while for the hydrometallurgical process route, an energy consumption of 1,472.4 MWh/a was determined.

Appendix C. Detailed sensitivity analysis charts

The scenario abbreviations used in the figures are composed of a part identifying the market development scenario (LM: lower, BM: base, UM, upper) and a part identifying the price development scenario (FP: fixed, LP: lower, BP: base, UP: upper).

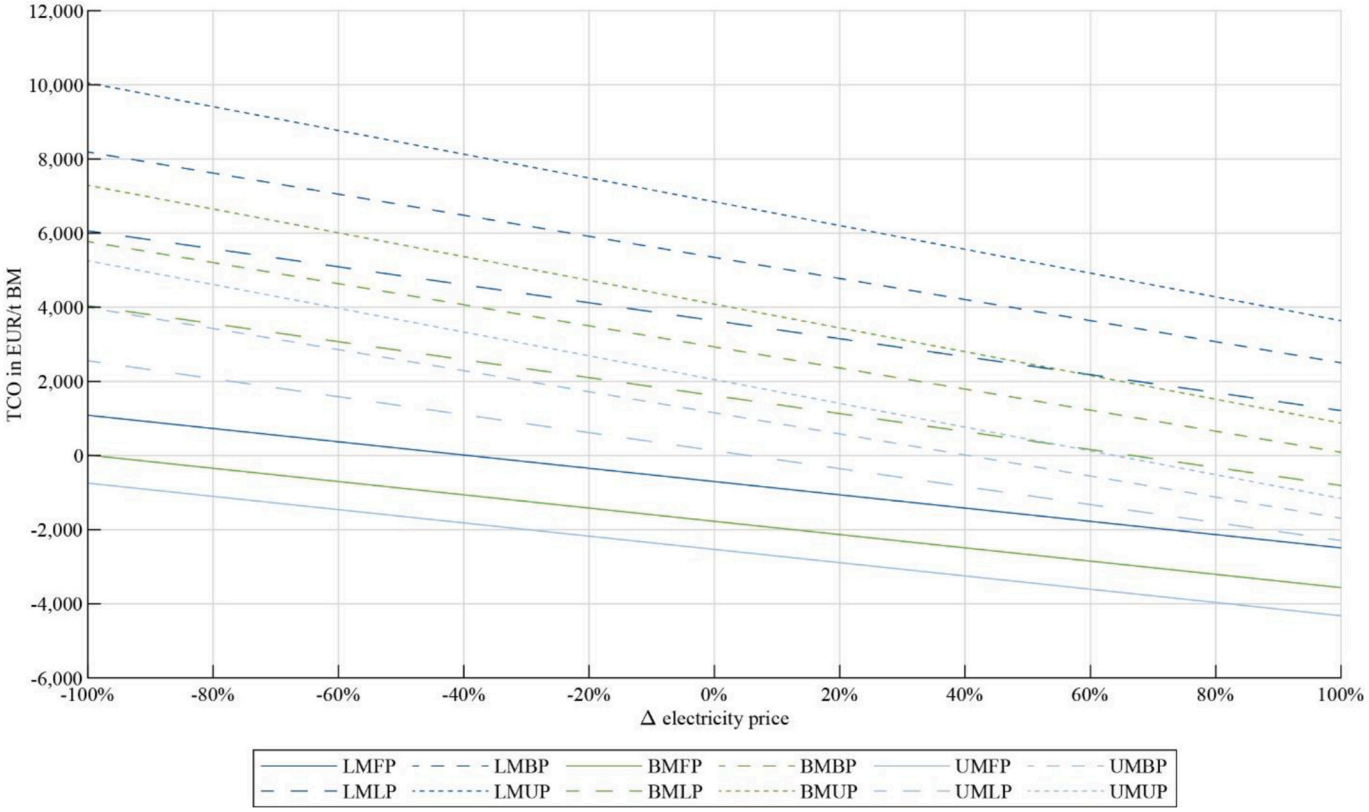

Fig. 6. Impact of the electricity base price on the TCO for all scenarios of the pyrometallurgical recycling route (own figure).

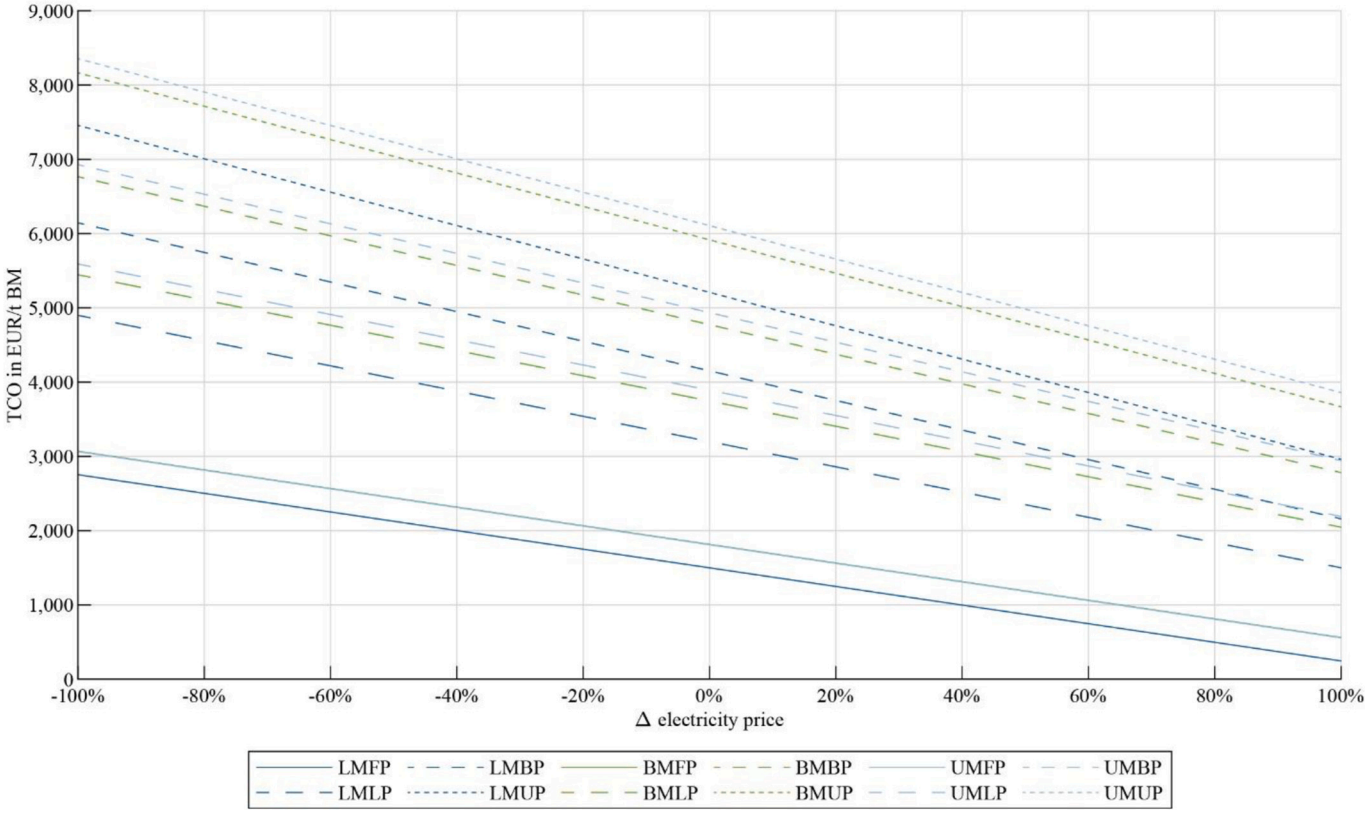

Fig. 7. Impact of the electricity base price on the TCO for all scenarios of the hydrometallurgical recycling route (own figure).

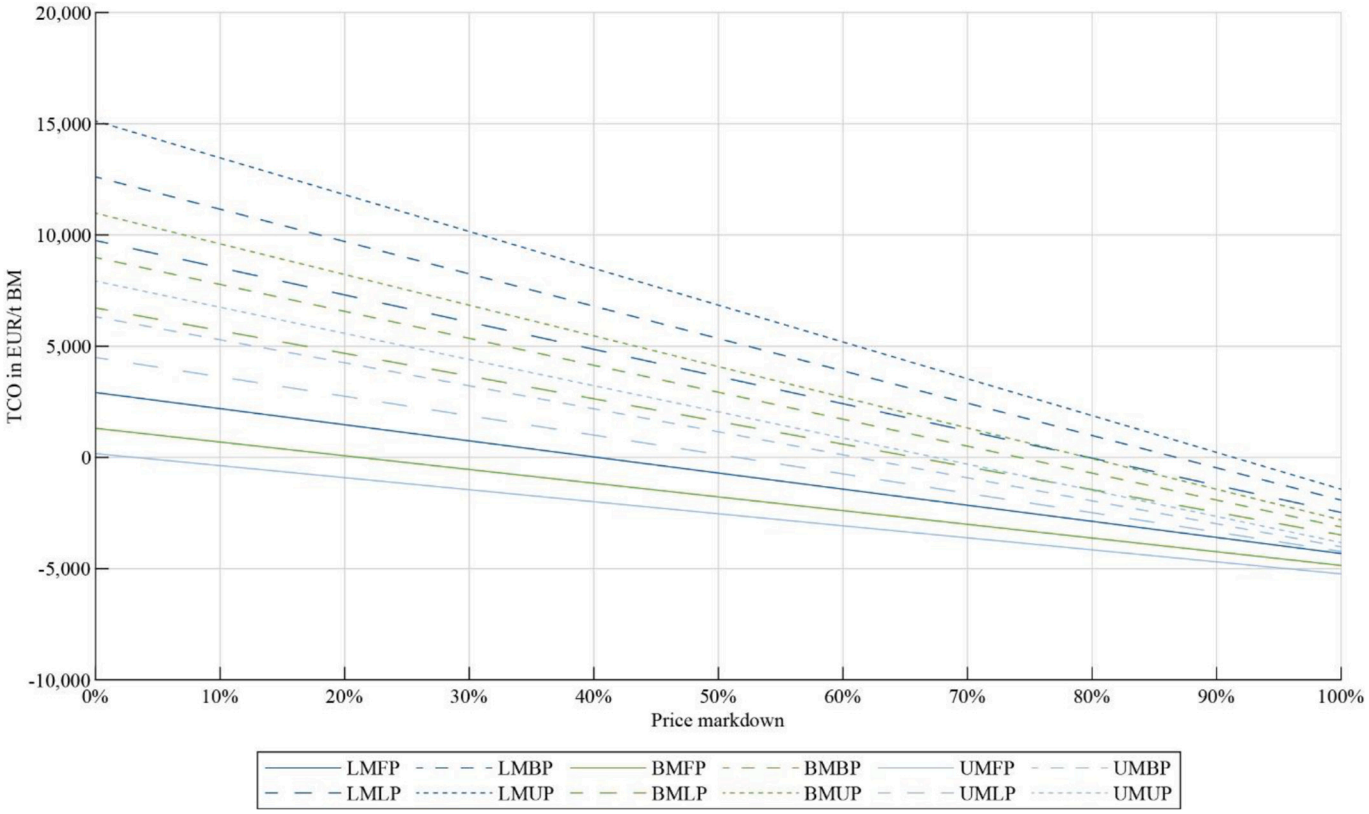

Fig. 8. Impact of the price markdown of the alloy on the TCO for all scenarios of the pyrometallurgical recycling route (own figure).

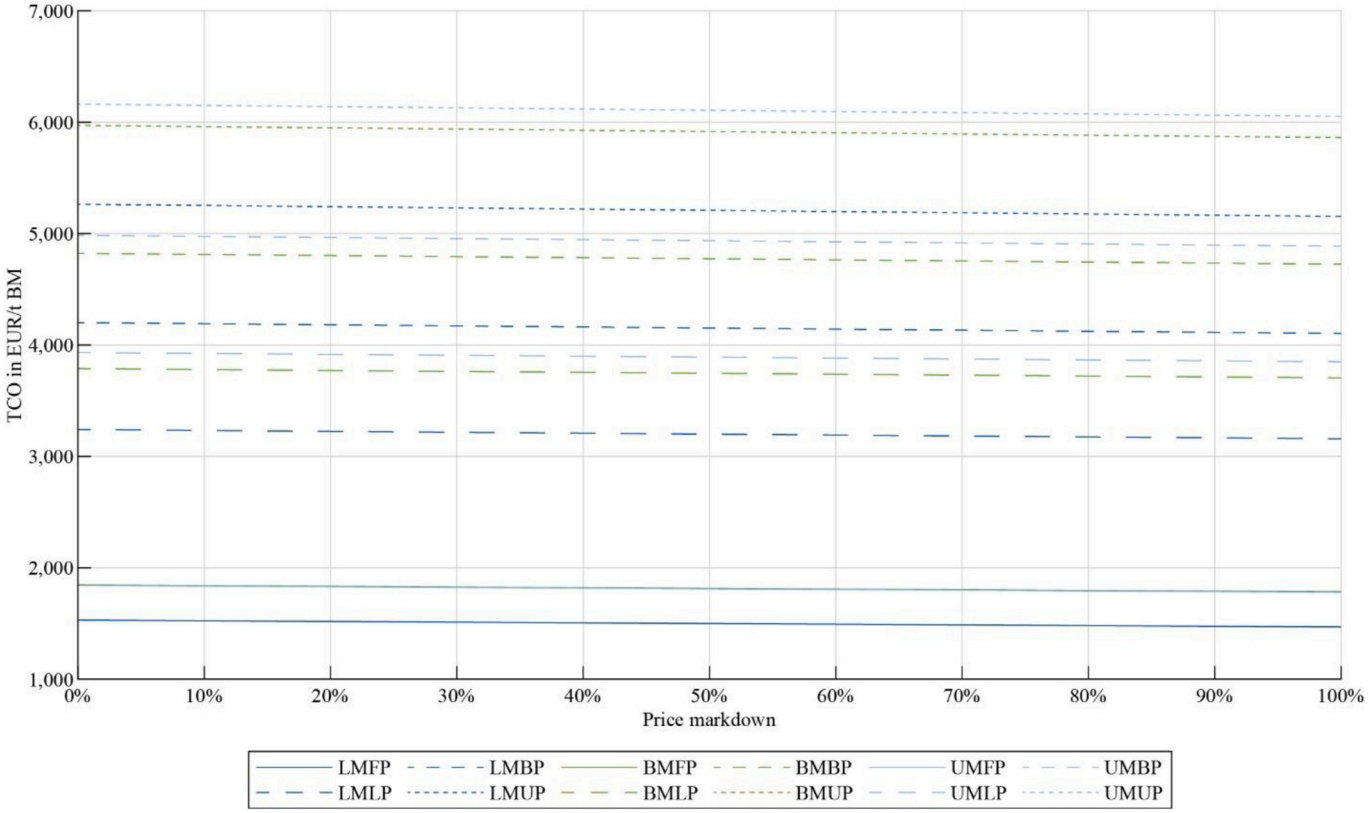

Fig. 9. Impact of the price markdown of cement Cu on the TCO for all scenarios of the hydrometallurgical recycling route (own figure).

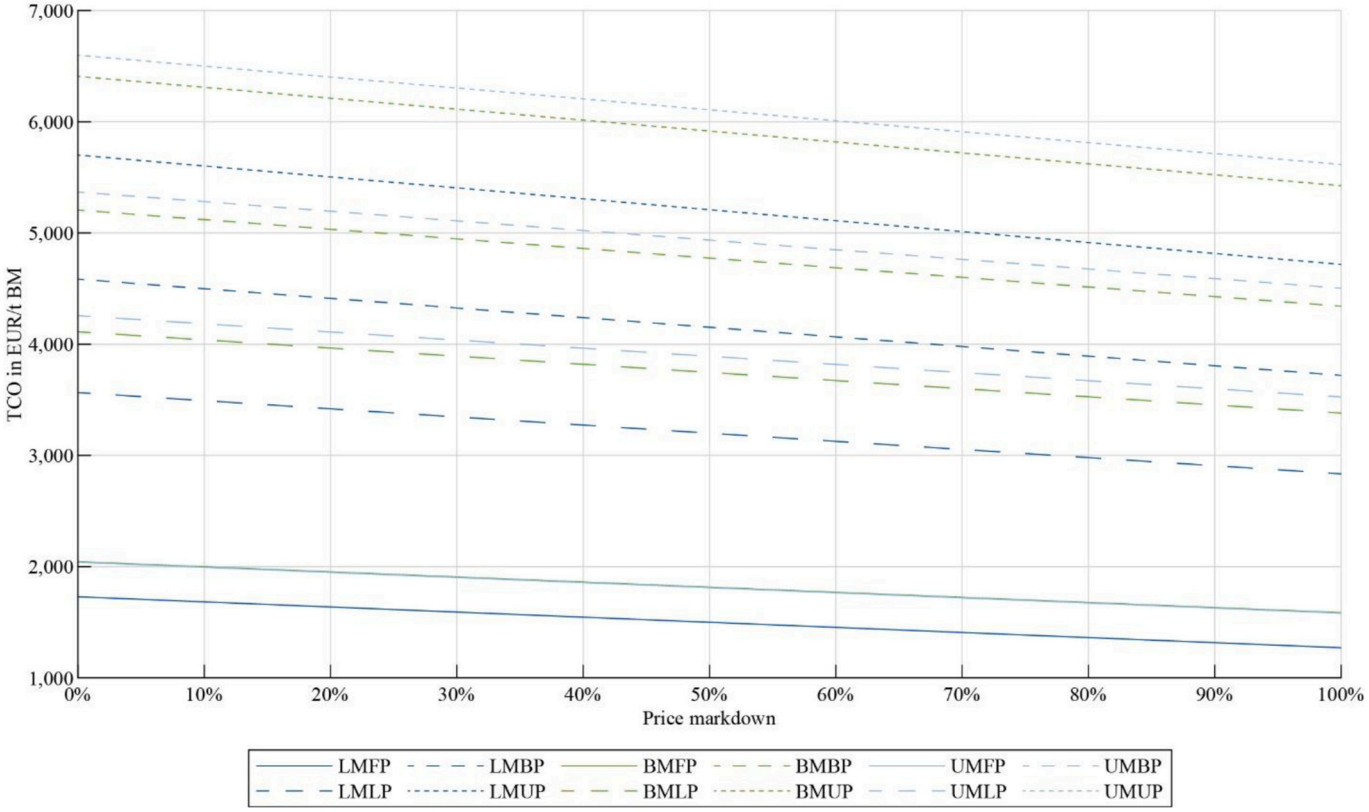

Fig. 10. Impact of the price markdown of Graphite on the TCO for all scenarios of the hydrometallurgical recycling route (own figure).

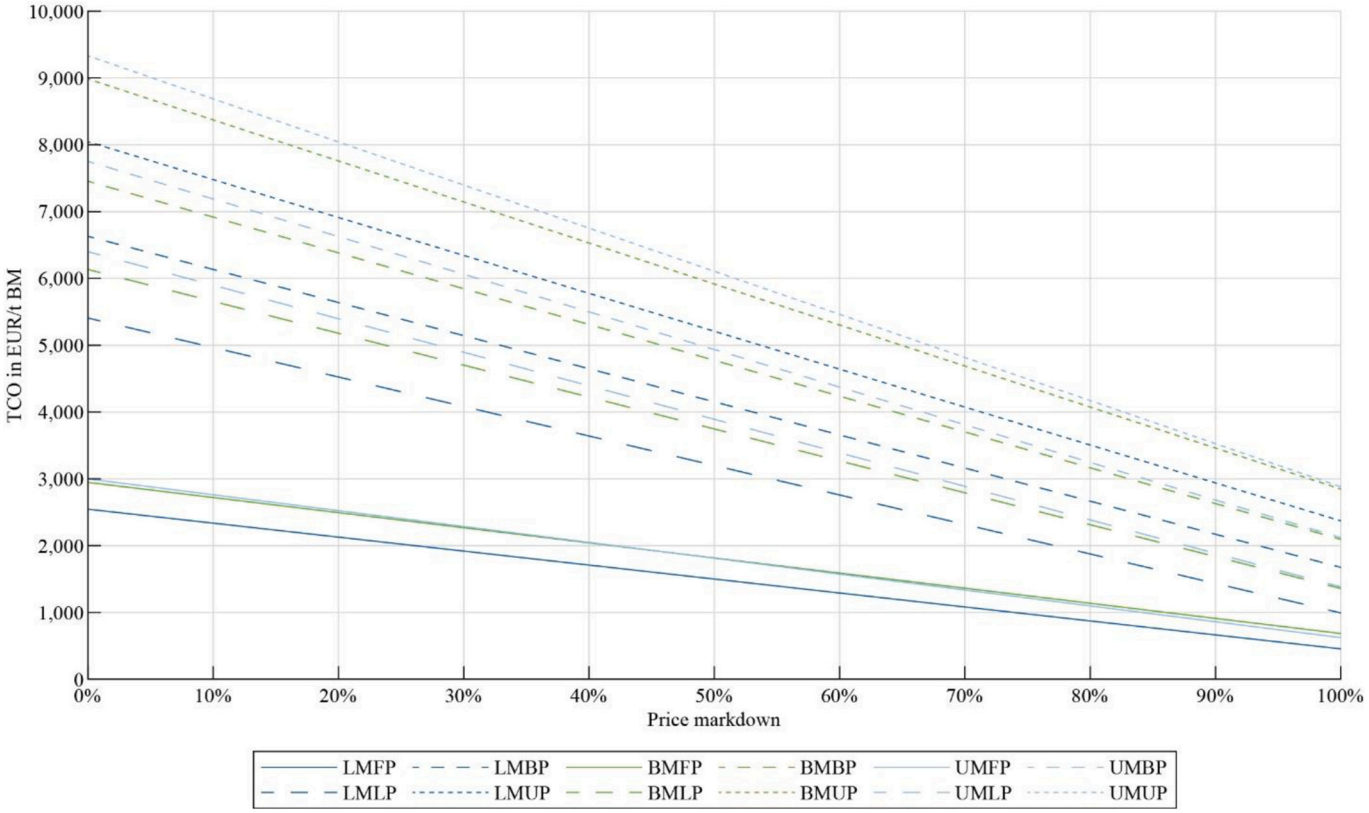

Fig. 11. Impact of the price markdown of Li_2CO_3 on the TCO for all scenarios of the hydrometallurgical recycling route (own figure).

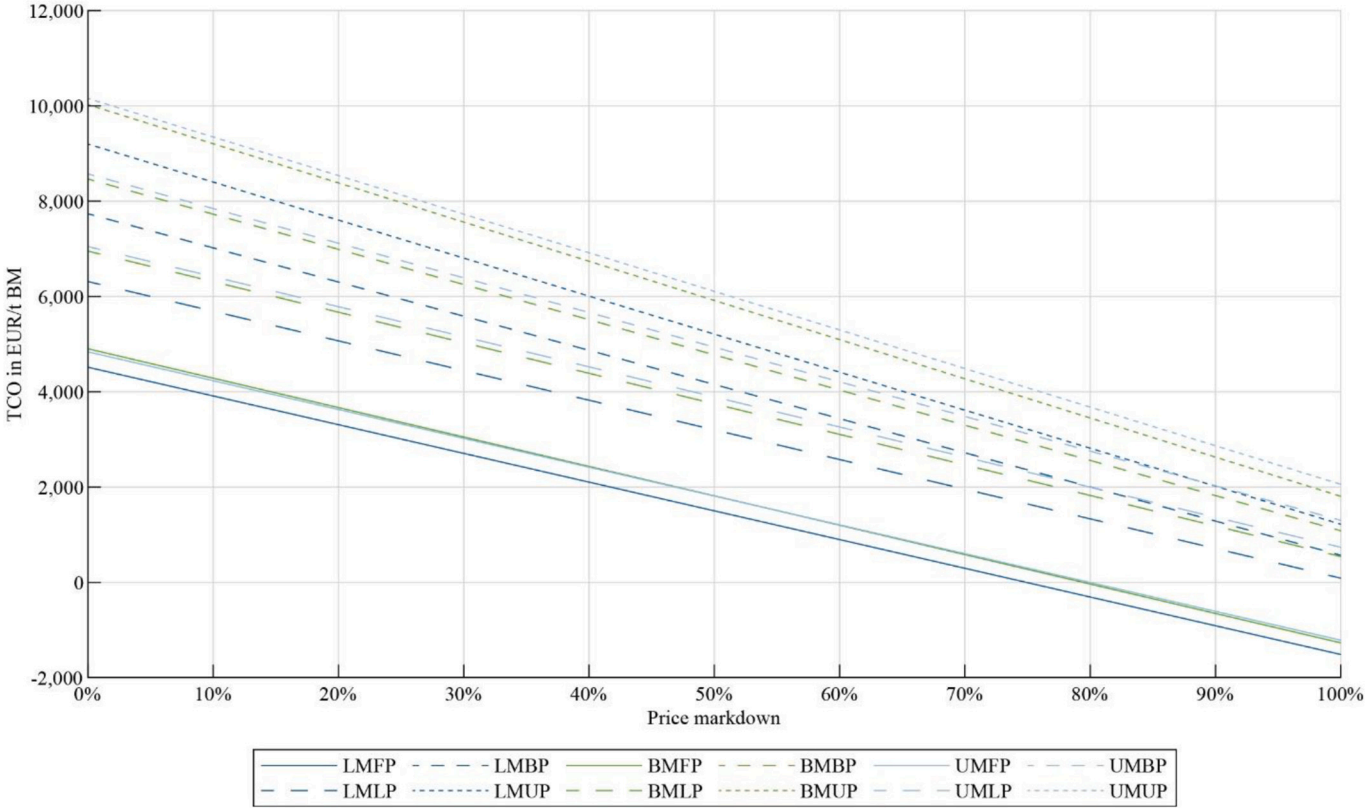

Fig. 12. Impact of the price markdown of Ni/Co/Mn hydroxide on the TCO for all scenarios of the hydrometallurgical recycling route (own figure).

References

[1] Accurec Recycling GmbH. Battery recycling datasheet. 2018. Available online at https://accurec.de/wp-content/uploads/2018/04/Li-ion-RE_2018.pdf, checked on 8/15/2023.

[2] Arnberger A, Coskun E, Rutrecht B. Recycling von Lithium-Ionen-Batterien. In: Thiel Stephanie, Thomé-Kozmiensky Elisabeth, Goldmann Daniel, editors. Recycling und Rohstoffe, vol. 11. Nietwerder: TKh2018 (Recycling und Rohstoffe, 11); 2018. p. 583–99.

[3] Azevedo M, Campagnol N, Hagenbruch T, Hoffmann K, Lala A, Ramsbottom O. Lithium and cobalt - a tale of two commodities. McKinsey&Company; 2018. Available online at https://www.mckinsey.com/~/media/mckinsey/industries/metals%20and%20mining/our%20insights/lithium%20and%20cobalt%20a%20tale%20of%20two%20commodities/lithium-and-cobalt-a-tale-of-two-commodities.pdf, checked on 9/8/2021.

[4] Bärwaldt G, Kwade A. LithoRec recycling von Lithium-Ionen-Batterien. In: Abschlussbericht zum Verbundvorhaben im Rahmen des FuE-Programms "Förderung von Forschung und Entwicklung im Bereich der Elektromobilität". Göttingen: Cuvillier Verlag; 2012.

[5] Bhutta KS, Huq F. Supplier selection problem: A comparison of the total cost of ownership and analytic hierarchy process approaches. In Supply Chain Manag 2002;7(3):126–35. https://doi.org/10.1108/13598540210436586.

[6] BKI - Baukosteninformationszentrum Deutscher Architektenkammern. Statistische Kostenkennwerte für Gebäude. With assistance of Hannes Spielbauer, Brigitte Kleinmann, Catrin Baumeister. Stuttgart: BKI Baukosteninformationszentrum (1). 2022.

[7] Blömeke S, Scheller C, Cerdas F, Thies C, Hachenberger R, Gonter M, et al. Material and energy flow analysis for environmental and economic impact assessment of industrial recycling routes for lithium-ion traction batteries. In J Cleaner Prod 2022;377:134344. https://doi.org/10.1016/j.jclepro.2022.134344.

[8] Blomgren GE. The development and future of lithium ion batteries. In J Electrochem Soc 2017;164(1):A5019–25. https://doi.org/10.1149/2.0251701jes.

[9] BMG - Bundesministerium für Gesundheit. Bekanntmachung des durchschnittlichen Zusatzbeitragssatzes nach § 242a Absatz 2 des Fünften Buches Sozialgesetzbuch für das Jahr 2022, revised 11/18/2021. Source: BAnz AT 30.11.2021 B4. 2021. Available online at https://www.bundesanzeiger.de/pub/publication/BRtmL7abzLxLOskV8An/content/BRtmL7abzLxLOskV8An/BAnz%20AT%2019.11.2021%20B4.pdf?inline, checked on 6/22/2023.

[10] BMUB - Bundesministerium für Umwelt, Naturschutz, Bau und Reaktorsicherheit. Klimaschutzplan 2050. Klimaschutzpolitische Grundsätze und Ziele der Bundesregierung. Berlin. 2016. Available online at https://www.bmwk.de/Redaktion/DE/Publikationen/Industrie/klimaschutzplan-2050.pdf, updated on 11/18/2022, checked on 7/7/2023.

[11] Bobba S, Carrara S, Huisman J, Mathieux F, Pavel C. Critical raw materials for strategic technologies and sectors in the EU. In: A Foresight Study Luxembourg: Publications Office of the European Union; 2020. https://doi.org/10.2873/58081.

[12] Brückner L, Frank J, Elwert T. Industrial recycling of lithium-ion batteries—A critical review of metallurgical process routes. In Metals (Basel) 2020;10(8):1107. https://doi.org/10.3390/met10081107.

[13] Bundesregierung Deutschland. Verordnung zur Bestimmung der Beitragssätze in der gesetzlichen Rentenversicherung für das Jahr 2018 (Beitragssatzverordnung 2018). BSV 2018, revised 12/18/2017. In Bundesgesetztblatt Teil I 2018;2017(79):3976.

[14] Campagnol N, Eddy J, Hagenbruch T, Klip D, Mulligan C, van de Staaij J. Metal mining constraints on the electric mobility horizon. McKinsey&Company; 2018. Available online at https://www.mckinsey.com/industries/oil-and-gas/our-insights/metal-mining-constraints-on-the-electric-mobility-horizon, updated on 4/1/2018, checked on 9/8/2021.

[15] Carrara S, Bobba S, Blagoeva D, Alves Dias P, Cavalli A, Georgitzikis K, et al. Supply chain analysis and material demand forecast in strategic technologies and sectors in the EU. In: A foresight study Luxembourg: Publications Office of the European Union; 2023. https://doi.org/10.2760/334074.

[16] Degraeve Z, Labro E, Roodhooft F. An evaluation of vendor selection models from a total cost of ownership perspective. In Eur J Oper Res 2000;125(1):34–58. https://doi.org/10.1016/S0377-2217(99)00199-X.

[17] Degraeve Z, Roodhooft F. Effectively selecting suppliers using Total cost of ownership. In J Supply Chain Manag 1999;35(1):5–10. https://doi.org/10.1111/j.1745-493X.1999.tb00050.x.

[18] DEHSt - German Emissions Trading Authority. Understanding national emissions trading. 2023. Available online at https://www.dehst.de/EN/national-emissions-trading/understanding-national-emissions-trading/understanding-nehs_node.html, checked on 6/22/2023.

[19] DERA - Deutsche Rohstoffagentur. Preismonitor Mai 2023. 2023. Available online at https://www.deutsche-rohstoffagentur.de/DERA/DE/Aktuelles/Monitore/2023/05-23/2023-05-preismonitor.pdf?_blob=publicationFile&v=2, checked on 6/22/2023.

[20] DERA - Deutsche Rohstoffagentur. Preistrendmonitor Januar 2023. 2023. Available online at https://www.deutsche-rohstoffagentur.de/DERA/DE/Aktuelles/Monitore/2023/01-23/2023-01-preistrendmonitor.pdf?_blob=publicationFile&v=3, checked on 6/22/2023.

[21] Destatis - Statistisches Bundesamt. 51000–0014: Aus- und Einfuhr (Außenhandel): Deutschland, Monate, Warenverzeichnis (8-Steller). 2023. Available online at https://www-genesis.destatis.de/genesis/online, checked on 3/30/2023.

[22] Deutscher Bundestag. Das Fünfte Buch Sozialgesetzbuch – Gesetzliche Krankenversicherung. SGB 5, revised 6/19/2023. In: In Bundesgesetztblatt Teil I 1988. 62; 1989. p. 2477.

[23] Deutscher Bundestag. Das Elfte Buch Sozialgesetzbuch – Soziale Pflegeversicherung. SGB 11, revised 6/19/2023. In: Bundesgesetztblatt Teil I 1994. 30; 1995. p. 1014.

[24] Deutscher Bundestag. Das Siebte Buch Sozialgesetzbuch – Gesetzliche Unfallversicherung. SGB 7, revised 6/19/2023. In: In *Bundesgesetztblatt Teil I* 1996. 43; 1997. p. 1254.

[25] Deutscher Bundestag. Das Dritte Buch Sozialgesetzbuch – Arbeitsförderung. SGB 3, revised 6/6/2023. In: In Bundesgesetztblatt Teil I 1997. 20; 1998. p. 594.

[26] Deutscher Bundestag. Bundes-Klimaschutzgesetz. KSG, revised 8/18/2021. In: In Bundesgesetztblatt Teil I 2019. 48; 2019. p. 2513.

[27] Ding Y, Cano ZP, Yu A, Lu J, Chen Z. Automotive Li-ion batteries: current status and future perspectives. In Electrochem Energy Rev 2019;2(1):1–28. https://doi.org/10.1007/s41918-018-0022-z.

[28] EEX - European Energy Exchange AG. Environmental Markets. 2023. Available online at https://www.eex.com/en/market-data/environmental-markets, checked on 3/31/2023.

[29] Ellram LM. A taxonomy of total cost of ownership models. In J Bus Logist 1994;15(1):171–91.

[30] Ellram LM. Total cost of ownership: an analysis approach for purchasing. In Int J Phys Dist Logist 1995;25(8):4–23. https://doi.org/10.1108/09600039510099928.

[31] Ellram LM, Siferd SP. Purchasing: the cornerstone of the total cost of ownership concept. In J Bus Logist 1993;14(1):163–84.

[32] Ellram LM, Siferd SP. Total cost of ownership: A key concept in strategic cost management decisions. In J Bus Logist 1998;19(1):55–84.

[33] Elwert T, Römer F, Schneider K, Hua Q, Buchert M. Recycling of batteries from electric vehicles. In: Pistoia Gianfranco, Liaw Boryann, editors. Behaviour of Lithium-ion batteries in electric vehicles. Cham: Springer International Publishing; 2018. p. 289–321. https://doi.org/10.1007/978-3-319-69950-9_12.

[34] EU - European Union. Directive 2003/87/EC of the European Parliament and of the Council of 13 October 2003 establishing a scheme for greenhouse gas emission allowance trading within the Community and amending Council Directive 96/61/EC. In *OJEU* 46 (L 275). 2003. p. 32–46. Available online at https://eur-lex.europa.eu/eli/dir/2003/87/oj, checked on 6/22/2023.

[35] EU - European Union. Directive 2006/66/EC of the European Parliament and of the Council of 6 September 2006 on batteries and accumulators and waste batteries and accumulators and repealing Directive 91/157/EEC. In *OJEU* 49 (L 266). 2006. p. 1–14. Available online at https://eur-lex.europa.eu/eli/dir/2006/66/oj, checked on 6/22/2023.

[36] EU - European Union. Directive 2009/29/EC of the European Parliament and of the Council of 23 April 2009 amending Directive 2003/87/EC so as to improve and extend the greenhouse gas emission allowance trading scheme of the Community. In *OJEU* 52 (L 140). 2009. p. 63–87. Available online at https://eur-lex.europa.eu/eli/dir/2009/29/oj, checked on 6/22/2023.

[37] EU - European Union. Commission Delegated Regulation (EU) 2019/331 of 19 December 2018 determining transitional Union-wide rules for harmonised free allocation of emission allowances pursuant to Article 10a of Directive 2003/87/EC of the European Parliament and of the Council. In *OJEU* 62 (L 59). 2019. p. 8–69. Available online at https://eur-lex.europa.eu/eli/reg_del/2019/331/oj, checked on 6/22/2023.

[38] European Commission. Critical Raw Materials Resilience: Charting a Path towards greater Security and Sustainability. Brussels. 2020. Available online at https://eur-lex.europa.eu/legal-content/EN/TXT/?uri=CELEX:52020DC0474, updated on 9/3/2020, checked on 6/22/2023.

[39] European Commission. Green Deal: EU agrees new law on more sustainable and circular batteries to support EU's energy transition and competitive industry. Brussels. 2022. Available online at https://ec.europa.eu/commission/presscorner/detail/en/IP_22_7588, updated on 12/9/2022, checked on 7/7/2023.

[40] Eurostat. Electricity prices for non-household consumers - bi-annual data (from 2007 onwards). Eurostat. 2023. Available online at https://ec.europa.eu/eurostat/databrowser/view/nrg_pc_205/default/table?lang=EN, updated on 6/20/2023, checked on 6/22/2023.

[41] Ferrin BG, Plank RE. Total cost of ownership models: an exploratory study. In J Supply Chain Manag 2002;38(3):18–29. https://doi.org/10.1111/j.1745-493X.2002.tb00132.x.

[42] Friedrich B, Peters L, Stallmeister C, Schier C. Innovative Lösungen für verbesserte Recyclingeffizienz bei der Verarbeitung von gebrauchten Li-Batterien. In: IME - Metallurgische Prozesstechnik und Metallrecycling RWTH Aachen; 2019. https://doi.org/10.13140/RG.2.2.13217.97123.

[43] Fujita T, Chen H, Wang K, He C, Wang Y, Dodbiba G, et al. Reduction, reuse and recycle of spent Li-ion batteries for automobiles: A review. In Int J Miner Metall Mater 2021;28(2):179–92. https://doi.org/10.1007/s12613-020-2127-8.

[44] Gaines L, Richa K, Spangenberger J. Key issues for Li-ion battery recycling. In MRS Energy Sustain 2018;5(1). https://doi.org/10.1557/mre.2018.13.

[45] Gaines LL, Dunn JB. Lithium-ion battery environmental impacts. In: Pistoia Gianfranco, editor. Lithium-ion batteries. Advances and applications. Amsterdam: Elsevier; 2014. p. 483–508. https://doi.org/10.1016/B978-0-444-59513-3.00021-2.

[46] Geissdörfer K, Gleich R, Wald A. Standardisierungspotentiale lebenszyklusbasierter Modelle des strategischen Kostenmanagements. In Z Betriebswirt 2009;79(6):693–715. https://doi.org/10.1007/s11573-009-0256-7.

[47] Georgi-Maschler T, Friedrich B, Weyhe R, Heegn H, Rutz M. Development of a recycling process for Li-ion batteries. In J Power Sources 2012;207:173–82. https://doi.org/10.1016/j.jpowsour.2012.01.152.

[48] Grohol M, Veeh C. Study on the critical raw materials for the EU 2023. In: Final Report Luxembourg: Publications Office of the European Union; 2023. https://doi.org/10.2873/725585.

[49] Gutsch M, Leker J. Costs, carbon footprint, and environmental impacts of lithium-ion batteries – from cathode active material synthesis to cell manufacturing and recycling. In Appl Energy 2024;353:122132. https://doi.org/10.1016/j.apenergy.2023.122132.

[50] Harper G, Sommerville R, Kendrick E, Driscoll L, Slater P, Stolkin R, et al. Recycling lithium-ion batteries from electric vehicles. In Nat 2019;575(7781):75–86. https://doi.org/10.1038/s41586-019-1682-5.

[51] Heimes H, Kampker A, Dorn B, Offermanns C, Bockey G, Wennemar S, et al. Battery Atlas 2022. In: Heimes Heiner, Wyboris Mischa, editors. Shaping the European Lithium-Ion Battery Industry. 1st ed. Aachen: PEM of RWTH Aachen University; 2022.

[52] Hu J, Zhang J, Li H, Chen Y, Wang C. A promising approach for the recovery of high value-added metals from spent lithium-ion batteries. In J Power Sources 2017;351:192–9. https://doi.org/10.1016/j.jpowsour.2017.03.093.

[53] IG Metall. Wie viel Urlaub steht mir zu? Urlaubsdauer und Urlaubsgeld. 2011. Available online at https://www.igmetall.de/tarif/tariftabellen/wieviel-urlaub-steht-mir-zu, updated on 11/11/2011, checked on 6/22/2023.

[54] IG Metall. Metall- und Elektroindustrie: ERA-Monatsentgelte. 2023. Available online at https://www.igmetall.de/download/20230328_28_33_MuE_ERA_Tabelle n_be6941718a1626188e4a7b826c32ba3295fe1391.pdf, checked on 6/22/2023.

[55] IG Metall. Metall- und Elektroindustrie: Zuschläge für Mehr-, Schicht-, Wechselschicht- und Nachtarbeit. 2023. Available online at https://www.igmetall.de/download/20230524_41_44_MuE_Zuschlaege_f0bb91d351583ac10e249e71661c1bdd1e98b6f2.pdf, checked on 6/22/2023.

[56] Julien CM, Mauger A. NCA, NCM811, and the route to Ni-richer lithium-ion batteries. In Energies 2020;13(23):6363. https://doi.org/10.3390/en13236363.

[57] Lander L, Tagnon C, Nguyen-Tien V, Kendrick E, Elliott RJ, Abbott AP, et al. Breaking it down: A techno-economic assessment of the impact of battery pack design on disassembly costs. In Appl Energy 2023;331:120437. https://doi.org/10.1016/j.apenergy.2022.120437.

[58] Marscheider-Weidemann F, Langkau S, Eberling E, Erdmann L, Haendel M, Krail M, et al. Raw materials for emerging technologies 2021. Berlin: DERA (DERA Rohstoffinformationen, 50). 2021. Available online at https://www.deutsche-rohstoffagentur.de/DE/Gemeinsames/Produkte/Downloads/DERA_Rohstoffinformationen/rohstoffinformationen-50-en.pdf, checked on 7/7/2023.

[59] Marshall J, Gastol D, Sommerville R, Middleton B, Goodship V, Kendrick E. Disassembly of Li ion cells—characterization and safety considerations of a recycling scheme. In Metals (Basel) 2020;10(6):773. https://doi.org/10.3390/met10060773.

[60] Martin G, Rentsch L, Höck M, Bertau M. Lithium market research – global supply, future demand and price development. In Energy Storage Mater 2017;6:171–9. https://doi.org/10.1016/j.ensm.2016.11.004.

[61] Miao Y, Hynan P, von Jouanne A, Yokochi A. Current Li-ion battery technologies in electric vehicles and opportunities for advancements. In Energies (Basel) 2019;12(6):1074. https://doi.org/10.3390/en12061074.

[62] Michaelis S, Schütrumpf J, Kampker A, Heimes H, Dorn B, Wennemar S, et al. Roadmap battery production equipment 2030. 2023. Update 2023. Available online at https://publica.fraunhofer.de/handle/publica/441379, checked on 6/30/2023.

[63] Monconduit L, Croguennec L, Dedryvère R. Electrodes for Li-Ion batteries. In: Materials, mechanisms and performance. Hoboken, NJ, USA: John Wiley & Sons, Inc; 2015. https://doi.org/10.1002/9781119007364.

[64] Mossali E, Picone N, Gentilini L, Rodrìguez O, Pérez JM, Colledani M. Lithium-ion batteries towards circular economy: A literature review of opportunities and issues of recycling treatments. In J Environ Manag 2020;264:110500. https://doi.org/10.1016/j.jenvman.2020.110500.

[65] Pinegar H, Smith YR. Recycling of end-of-life Lithium ion batteries, part I: commercial processes. In J Sustain Metall 2019;5(3):402–16. https://doi.org/10.1007/s40831-019-00235-9.

[66] PwC - PricewaterhouseCoopers GmbH. Materials. 2022. Available online at https://pwc-tools.de/kapitalkosten/en/materials/, checked on 1/19/2023.

[67] Reinhart L, Vrucak D, Woeste R, Lucas H, Rombach E, Friedrich B, et al. Pyrometallurgical recycling of different lithium-ion battery cell systems: economic and technical analysis. In J Cleaner Prod 2023;416:137834. https://doi.org/10.1016/j.jclepro.2023.137834.

[68] Repenning J, Harthan R, Blanck R, Böttcher H, Braungardt S, Bürger V, et al. Klimaschutzinstrumente-Szenario 2030 (KIS-2030) zur Erreichung der Klimaschutzziele 2030. Edited by Umweltbundesamt (Climate Change, 30). 2023. Available online at https://www.umweltbundesamt.de/publikationen/klimaschutzinstrumente-szenario-2030-kis-2030-zur, checked on 7/7/2023.

[69] Schmuch R, Wagner R, Hörpel G, Placke T, Winter M. Performance and cost of materials for lithium-based rechargeable automotive batteries. In Nat Energy 2018;3(4):267–78. https://doi.org/10.1038/s41560-018-0107-2.

[70] Schulz KJ, DeYoung JH, Seal RR, Bradley DC. Critical mineral resources of the United States - Economic and environmental geology and prospects for future supply. In: U.S. Geological Survey Professional Paper 1802. Reston (VA): U.S. Department of the Interior U.S. Geological Survey (Professional paper / U.S. Department of the Interior, U.S. Geological Survey, 1802); 2017. https://doi.org/10.3133/pp1802.

[71] Schwich L, Schubert T, Friedrich B. Early-stage recovery of Lithium from tailored thermal conditioned black mass part I: mobilizing Lithium via supercritical CO2-carbonation. In Metals (Basel) 2021;11(2):177. https://doi.org/10.3390/met11020177.
[72] SMM - Shanghai Metals Market. Shanghai Metals Market. 2023. Available online at https://www.metal.com/, checked on 4/3/2023.
[73] Sommerfeld M, Vonderstein C, Dertmann C, Klimko J, Oráč D, Miškufová A, et al. A combined pyro- and hydrometallurgical approach to recycle pyrolyzed lithium-ion battery black mass part 1: production of Lithium concentrates in an electric arc furnace. In Metals (Basel) 2020;10(8):1069. https://doi.org/10.3390/met10081069.
[74] Stallmeister C, Schwich L, Friedrich B. Early-Stage Li-Removal. Vermeidung von Lithiumverlusten im Zuge der Thermischen und Chemischen Recyclingrouten von Batterien. In: Elisabeth Thomé-Kozmiensky, Olaf Holm, Bernd Friedrich, Daniel Goldmann (Eds.): Recycling und Sekundärrohstoffe, vol. 13. Berliner Recycling- und Sekundärrohstoffkonferenz. Nietwerder: Thomé-Kozmiensky Verlag GmbH (Recycling und Rohstoffe, 13); 2020. p. 544–57.
[75] Statista. Market share of different types of electric vehicle (EV) cathode chemistries in 2020 with a forecast for 2025 through 2050. Statista Inc; 2021. Available online at https://www.statista.com/statistics/1248519/distribution-of-different-electric-vehicle-batteries-on-the-global-market/, checked on 9/8/2021.
[76] Statista. Projected global battery demand from 2020 to 2030, by application. Statista Inc; 2021. Available online at https://www.statista.com/statistics/1103218/global-battery-demand-forecast/, checked on 6/27/2023.
[77] Statista. Projected size of the global lithium-ion battery market from 2020 to 2026 (in billion U.S. dollars). Statista Inc; 2021. Available online at https://www.statista.com/statistics/1011187/projected-global-lithium-ion-battery-market-size/, checked on 9/8/2021.
[78] Stawag - Stadtwerke Aachen AG. Wasserlieferungsabkommen. Preisblatt zur Belieferung mit Wasser. 2021. Available online at https://www.stawag.de/file admin/stawag/content/Dokumente/Preise_Mwst/PB_Wasserlieferungsabkommen.pdf, checked on 3/31/2023.
[79] Thielmann A, Neef C, Hettesheimer T, Döscher H, Wietschel M, Tübke J. Energiespeicher-Roadmap (Update 2017). Hochenergie-Batterien 2030+ und Perspektiven zukünftiger Batterietechnologien. Fraunhofer ISI - Fraunhofer-Institut für System- und Innovationsforschung ISI. Karlsruhe. 2017. Available online at http://publica.fraunhofer.de/documents/N-481231.html, checked on 9/8/2021.
[80] Vekić N. Lithium-Ionen-Batterien für die Elektromobilität: Status. Zukunftsperspektiven, Recycling: Thinktank Industrielle Ressourcenstrategien; 2020. https://doi.org/10.13140/RG.2.2.14824.70406.
[81] Velázquez-Martínez O, Valio J, Santasalo-Aarnio A, Reuter M, Serna-Guerrero R. A critical review of Lithium-ion battery recycling processes from a circular economy perspective. In Batteries (Basel) 2019;5(4):68. https://doi.org/10.3390/batteries5040068.
[82] Vest M. Weiterentwicklung des pyrometallurgischen IME Recyclingverfahrens für Li-Ionen Batterien von Elektrofahrzeugen. Dissertation. Aachen: Shaker Verlag GmbH Schriftenreihe des IME, 42. 2016.
[83] Vezzini A. Manufacturers, materials and recycling technologies. In: Pistoia Gianfranco, editor. Lithium-ion batteries. Advances and applications. Amsterdam: Elsevier; 2014. p. 529–51. https://doi.org/10.1016/B978-0-444-59513-3.00023-6.
[84] Wang H. Development of a high efficient hydrometallurgical recycling process for automotive Li-ion batteries. In: Dissertation. With assistance of Bernd Friedrich, Daniel Goldmann, Stefan Luidold. Aachen: Shaker Verlag GmbH; 2015 [Schriftenreihe des IME, 36].
[85] Wang H, Friedrich B. Development of a highly efficient hydrometallurgical recycling process for automotive Li–ion batteries. In J Sustainable Metall 2015;1(2):168–78. https://doi.org/10.1007/s40831-015-0016-6.
[86] Yi W-T, Yan C-Y, Ma P-H. Kinetic study on carbonation of crude Li2CO3 with CO2-water solutions in a slurry bubble column reactor. In Korean J Chem Eng 2011;28(3):703–9. https://doi.org/10.1007/s11814-010-0405-2.